

# Acceleration of particles in spacetimes of black string

Arman Tursunov<sup>1,2,3,\*</sup>, Martin Kološ<sup>3,†</sup>, Ahmadjon Abdujabbarov<sup>1,2,‡</sup>,  
Bobomurat Ahmedov<sup>1,2,§</sup> and Zdeněk Stuchlík<sup>3¶</sup>

<sup>1</sup> Institute of Nuclear Physics, Ulughbek, Tashkent 100214, Uzbekistan

<sup>2</sup> Ulugh Begh Astronomical Institute, Astronomicheskaya 33, Tashkent 100052, Uzbekistan

<sup>3</sup> Institute of Physics, Faculty of Philosophy and Science, Silesian University in Opava,  
Bezručovo nám.13, CZ-74601 Opava, Czech Republic

The particle acceleration mechanism in  $S^2 \times \mathbb{R}^1$  topology, namely, in the spacetime of the five-dimensional compact black string, has been studied. The expression of center-of-mass energy of the colliding neutral particles near static black string has been found. The collision of a charged particle moving at the innermost stable circular orbit with a neutral particle coming from infinity has been considered when black string is immersed in external uniform magnetic field. It has been shown that the unlimited center-of-mass energy can be approached in the case of the extremal rotation of the black string which is similar to the analogous effect in Kerr spacetime. We have also obtained that the scattering energy of particles in the center-of-mass system can take arbitrarily large values not only for extremal black string but also for the nonextremal one. It has been derived that the presence of the extra dimension can, in principle, increase the upper limit of efficiency of energy extraction from the extremely rotating black string up to 203% versus 143% which can be extracted from the extreme Kerr black hole.

PACS numbers: 04.70.Bw, 04.50.Gh, 04.25.-g  
Keywords:

## I. INTRODUCTION

String theories give an infinite series of corrections to the theory of gravity and consequently more types of symmetries than those commonly assumed in standard Einstein general relativity. The bigger number of symmetries can be separated by the range of horizon topologies. The event horizon of the four-dimensional black hole is topologically spherical  $S^2$ , since the cross-section of the event horizon is a two-sphere while for 5D black holes the topology of the horizon is  $S^3$ . However, for a spacetime with one extra dimension, which is compactified to the circle with length  $2\pi L$ , the spacetime has  $S^2 \times \mathbb{R}^1$  topology [1]. This one-dimensional extended object surrounded by a horizon we will call *black string* [2].

It has been recently shown that new interesting properties of the geodesic motion occur if one adds the extra dimension to Schwarzschild or Kerr spacetimes [3]. When the additional dimension  $w$  is included to the well known four-dimensional Schwarzschild spacetime metric, the obtained solution will give us the spacetime metric of a five-dimensional static black string. By the same way one may obtain the spacetime metric for the rotating black string adding extra dimension to the spacetime of Kerr black hole [2].

One can use the following notations:

$$X^\alpha = (x^a, w), \quad \alpha = 0, 1, 2, 3, 4, \quad a = 0, 1, 2, 3 \quad (1)$$

for the complete set of coordinates which cover the spacetime. The coordinates  $x^\mu$  form the four-dimensional spacetime with metric  $g_{\mu\nu} = (-, +, +, +)$ . Then, the spacetime metric of the black string living in five dimensions takes the following form:

$$ds^2 = g_{\mu\nu} dx^\mu dx^\nu + dw^2, \quad (2)$$

where  $g_{\mu\nu} dx^\mu dx^\nu$  can be a metric of any four-dimensional black hole spacetime.

The existence of higher dimensions, which are mostly assumed to be compact, is essential for the intrinsic congruency of the field theory. Charged rotating black holes are considered in [4], while optical phenomena in the field of rotating black hole in braneworld has been studied in [5]. Equatorial circular orbits and the motion of the shell of dust in the field of a rotating naked singularity have been studied in detail in [6].

Observational possibilities of testing the braneworld black hole models at an astrophysical scale have been intensively discussed in the literature during the last several years, for example, through the gravitational lensing [7], the motion of test particles [8–10], and the classical tests of general relativity (perihelion precession, deflection of light, and the radar echo delay) in the Solar System (see, e.g., Ref. [11]). The energy flux, the emission spectrum, and accretion efficiency from the accretion disks around several classes of static and rotating braneworld black holes have been obtained in [12]. The complete set of analytical solutions of the geodesic equation of massive test particles in higher dimensional

\*Electronic address: arman@astrin.uz

†Electronic address: martin.kolos@fpf.slu.cz

‡Electronic address: ahmadjon@astrin.uz

§Electronic address: ahmedov@astrin.uz

¶Electronic address: zdenek.stuchlik@fpf.slu.cz

spacetimes which can be applied to braneworld models is provided in the recent paper [13].

The geodesic motion of test particles in the spacetimes of static and rotating black strings and in the various spacetimes related to cosmic strings have been studied in detail in the recent paper [3] and in [14–18]. The dynamics of a test particle in the spacetimes of Schwarzschild and Kerr black holes pierced by string has been studied in papers [19, 20], which was mentioned in [3]. Moreover, the solutions of the dynamical equations in the gravitational field of cosmic strings, such as Abelian-Higgs strings [21], two interacting Abelian-Higgs strings [22], and cosmic superstrings [23] were mentioned in the paper [3].

It has been shown by Bañados, Silk and West (BSW) [24] that a rotating axially symmetric black hole can act as a particle accelerator to arbitrarily high energies in the center-of-mass frame of the collision of a pair of particles. In particular, the BSW effect takes place when particles have the properly chosen values of angular momentum. Nowadays, the effect of infinite energy in the center-of-mass frame due to the collision of particles attracts much attention; see, e.g., [25]–[32]. It seems that this effect has a quite general character. The acceleration of particles by a spinning black hole [26], cylindrical black hole [25], weakly magnetized black hole [30], black hole with gravitomagnetic charge [31], or Kerr naked singularity [33] has been analyzed regarding the possibility of the production of the particles with unlimited energies. Energetic processes in the superspinning Kerr spacetimes have been also studied in papers [34–36]. By constructing escape null cones, it has been explicitly demonstrated that the high energy collisions occurring in the field of near extreme Kerr superspinars can be directly observed by distant observers [37]. Optical phenomena related to the appearance of Keplerian accretion discs orbiting Kerr superspinars have been studied in Ref. [38] Black hole production from ultrarelativistic collisions is explored in Ref. [39, 40]. Collision of particles in different trajectories are considered in [41, 42]. High energy collision of particles in the vicinity of black holes in higher dimensions have been studied in Ref. [43]. Efficiency of the particle collision and upper limit of energy extraction for Kerr black hole through particle acceleration are studied in [44, 45]. The particle acceleration around 5 dimensional rotating black hole in supergravity theory has been considered in recent paper [46]

In the present paper, our aim is to show that a similar effect of particle collision with high center-of-mass energy is also possible when the string theory phenomena are included. Namely, in the simplest case when a space dimension is added to the four-dimensional black hole solutions, it can be represented as the spacetime of black string (see, Fig.1)

The paper is organized as follows: in Sec. II the test particles motion as well as their acceleration near non-rotating 5D black string is studied. The Section III is

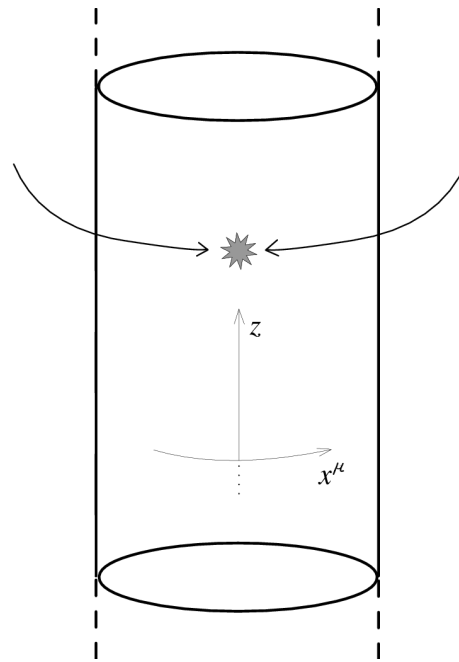


Figure 1: Schematic picture of two particles colliding near the event horizon of a black string.

devoted to investigation of charged particle motion and acceleration of particles around black string in external magnetic field. The rotating black string as particle accelerator is explored in Sec. IV. The energy extraction efficiency is studied in subsequent Sec. V. We conclude our results in Sec. VI.

Throughout the paper, we use a plus signature and a system of geometric units in which  $G = 1 = c$ . However, for those expressions with an astrophysical application, we have written the speed of light explicitly.

## II. BLACK STRING AS ACCELERATOR OF NEUTRAL PARTICLES

### A. Dynamical equations

Now, the geodesic motion of a test neutral particle in the spacetime of nonrotating black string will be studied. In addition, we will find the analytical solutions of the equations of motion and show the representative trajectories of a test particle in the vicinity of nonrotating black string.

When the additional dimension  $w$  is included to the metric of the Schwarzschild spacetime, the obtained solution takes the following form [3]

$$ds^2 = -\left(1 - \frac{2M}{r}\right) dt^2 + \left(1 - \frac{2M}{r}\right)^{-1} dr^2 + r^2(d\vartheta^2 + \sin^2\vartheta d\varphi^2) + dw^2, \quad (3)$$

where  $M$  is the mass density of the black string or the

mass per unit length. The solution 3 is the solution of a neutral uniform black string spacetime and the singularity is placed at the position  $r = 0$ . The event horizon is at the position  $r_H = 2M$ .

Consider the geodesic motion of a neutral point particle in the spacetime of the nonrotating static black string given by the expression (3). In order to find the trajectory of a particle one can use the Hamilton-Jacobi equation in the general form [3]

$$\frac{\partial S}{\partial \lambda} + \frac{1}{2} g^{\mu\nu} \frac{\partial S}{\partial x^\mu} \frac{\partial S}{\partial x^\nu} = 0, \quad (4)$$

where we parameterize by  $\lambda$  being an affine parameter of the geodesic line of the test particle.

The Hamiltonian of the test particle then can be written in the form

$$2H = g_{(4)}^{ab} P_a P_b + P_w^2 + m^2, \quad (5)$$

where the momenta of the particle are associated with the first derivative of the Hamilton-Jacobi action,  $S$ , with respect to the corresponding coordinate as  $P_\mu = \partial S / \partial x^\mu$ . The term  $g_{(4)}^{ab}$  denotes the four-dimensional part of the space-time metric (3).

Due to the symmetries of the background spacetime of a nonrotating black string, there are three constants of motion for each particle, which means there are three conserved quantities for any geodesic motion, namely, the energy  $E$ , the angular momentum  $L$ , and a new constant of motion  $J$ , which is related to the extra dimension  $w$ . The constants of the motion are related to the five-momentum as follows:

$$P_t = -E, \quad P_\varphi = L, \quad P_w = J. \quad (6)$$

One may look for the separable solutions of the Hamilton-Jacobi equations decomposing the action in the form [3]

$$S = \frac{1}{2} m_0^2 \lambda - Et + L\varphi + Jw + S_r(r). \quad (7)$$

To study the motion of test particles in the black string spacetime it is convenient to use the fact that the entire trajectory must lie on the plane if the initial position and the tangent vector to the trajectory of the particle lie on a plane that contains the center of the gravitating body. Without loss of generality we may therefore restrict ourselves to the study of equatorial trajectories with  $\vartheta = \pi/2$ . Hereafter, we set  $\vartheta = \pi/2$ , since the orbits always lie in a plane which can be selected as equatorial one. Substituting (7) into (4) and using (3), one can find the radial part of the action (7) in the form

$$S_r = \int \left[ \left( 1 - \frac{2M}{r} \right)^{-2} E^2 - \left( 1 - \frac{2M}{r} \right)^{-1} \left( \frac{L^2}{r^2} + J^2 + m^2 \right) \right]^{1/2} r \quad (8)$$

Let us denote for convenience [3]

$$\mathcal{E} = \frac{E}{m}, \quad \mathcal{L} = \frac{L}{m}, \quad \mathcal{J} = \frac{J}{m}, \quad (9)$$

where  $\mathcal{E}$ ,  $\mathcal{L}$ , and  $\mathcal{J}$  are the specific energy, angular momentum and new constant of motion per unit of mass  $m$  of the particle.

Then the Hamilton-Jacobi equation (4) can be separated and gives the equations of motion in differential form for each component as

$$\frac{dt}{d\tau} = \mathcal{E} \left( 1 - \frac{2M}{r} \right)^{-1}, \quad (10)$$

$$\frac{d\varphi}{d\tau} = \frac{\mathcal{L}}{r^2}, \quad (11)$$

$$\frac{dw}{d\tau} = \mathcal{J}, \quad (12)$$

$$\left( \frac{dr}{d\tau} \right)^2 = \mathcal{E}^2 - \left( 1 - \frac{2M}{r} \right) \left( 1 + \frac{\mathcal{L}^2}{r^2} + \mathcal{J}^2 \right). \quad (13)$$

The integral of motion  $\mathcal{J}$  which is related to the symmetry of the extra dimension  $w$ , appears in the  $r$  and  $w$  equations, (13) and (12), respectively, while remaining equations do not change their original form presented in the four-dimensional Schwarzschild spacetime [3]. The equations of motion (10)-(13) are invariant under the following reversals of signs

$$\mathcal{L} \rightarrow -\mathcal{L}, \quad \varphi \rightarrow -\varphi, \quad (14)$$

and

$$\mathcal{J} \rightarrow -\mathcal{J}, \quad w \rightarrow -w, \quad (15)$$

## B. Effective potential of the motion

The number of turning points and the form of the effective potential allow us to define the possible orbits in the given spacetime. In the nonrotating black string vicinity there exist: terminating orbits (TO), for which the trajectory of a particle ends in singularity, escape orbits (EO), where the trajectories are open to infinity, and bound orbits (BO), where the trajectories are closed [3]. Depending on the type of orbit, the possible trajectories cover all region between  $[0, \infty)$ .

Let us introduce the effective potential  $V_{\text{eff}}$

$$V_{\text{eff}} = \left( 1 - \frac{2M}{r} \right) \left( 1 + \frac{\mathcal{L}^2}{r^2} + \mathcal{J}^2 \right) \quad (16)$$

which can be easily defined from Eq. (13) as

$$\left( \frac{dr}{d\tau} \right)^2 = \mathcal{E}^2 - V_{\text{eff}}. \quad (17)$$

In the asymptotical infinity  $r \rightarrow \infty$ , or in the flat spacetime limit, the effective potential  $V_{\text{eff}}$  takes the value

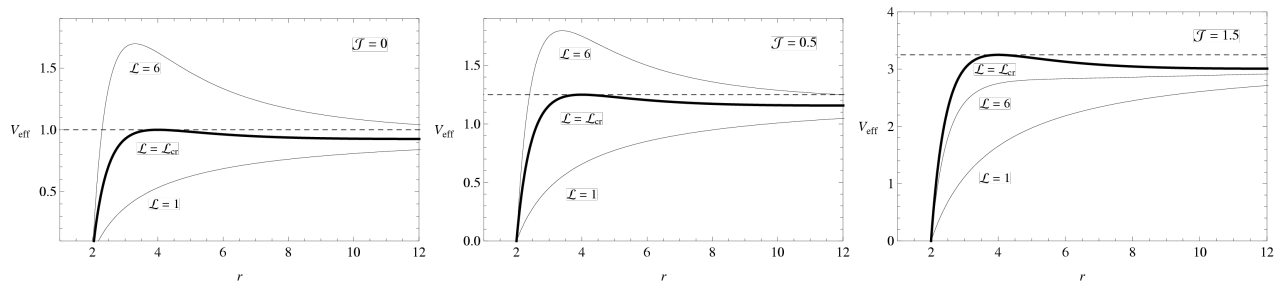


Figure 2: Effective potential of the motion for the different values of parameters  $\mathcal{L}$  and  $\mathcal{J}$ . Thick solid curves correspond to the particles with the critical angular momentum  $\mathcal{L}_{\text{cr}}$  while dashed lines are the levels of the energy of a free particle at infinity. Thin solid curves are the potentials of the particles with the representative values of the angular momentum  $\mathcal{L} = 1$  and  $\mathcal{L} = 6$ .

$1 + \mathcal{J}^2$ . In the opposite limiting case  $r \rightarrow 0$ , the effective potential diverges,  $V_{\text{eff}} \rightarrow -\infty$  [3]. Equation (17) also determines the turning points of an orbit. The shapes of the effective potential for representative values of  $\mathcal{L}$  and  $\mathcal{J}$  are shown in Fig.2.

The type of the motion depends on the number of the turning points i.e. on the number of extrema of the effective potential. The extremum of the effective potential lies at

$$r_{\text{ext}} = \frac{\mathcal{L}^2 \pm \mathcal{L}\sqrt{\mathcal{L}^2 - 12(1 + \mathcal{J}^2)}}{2(1 + \mathcal{J}^2)}. \quad (18)$$

Hereafter we set the mass density of the black string as  $M = 1$ . It is obvious from (18) that the condition of the presence of the extrema of the effective potential corresponds to the positive values of the radicand of (18), which gives

$$|\mathcal{L}| > 2\sqrt{3}\sqrt{1 + \mathcal{J}^2}. \quad (19)$$

Numbers of extrema define the possibility of the existence of turning points. The samples of the trajectories are shown in Fig. 3 for the different values of parameter  $\mathcal{J}$ .

### C. Freely falling particle

Consider a neutral particle freely falling from infinity at rest in the direction of an event horizon of the static black string. The final state of the particle entirely depends on its momenta  $\mathcal{L}$  and  $\mathcal{J}$ . If the angular momentum of the particle  $\mathcal{L}$  is larger than maximum critical value, then the geodesics of the particle may never reach the vicinity of the horizon and the strong gravitational effects cannot be analyzed. On the other hand, for the small values of angular momentum, the particles fall radially with a small tangential velocity and the center-of-mass energy does not grow either. Consequently, there is a critical value for the angular momentum such that particles may reach the horizon with maximum tangential velocity. The energy of the particle at rest at infinity corresponds to its energy in flat spacetime

$$\mathcal{E}^2 = 1 + \mathcal{J}^2, \quad (20)$$

which is in contrast with the value  $\mathcal{E}_{(4D)} = 1$  defined in four-dimensional spacetime. To find the value of the critical angular momentum one can rewrite Eq. (13) using (20) in the form

$$\frac{dr}{d\tau} = \dot{r} = \pm \frac{1}{r^2} \sqrt{2r^3(1 + \mathcal{J}^2) - \mathcal{L}^2 r(r - 2)}. \quad (21)$$

The dependence of  $\dot{r}$  on the radial coordinate  $r$  for different values of  $\mathcal{L}$  and  $\mathcal{J}$  is shown in Fig.4. It is obvious from Fig. 4 that there is a critical value of the angular momentum

$$\mathcal{L}_{\text{cr}} = \pm 4\sqrt{1 + \mathcal{J}^2}, \quad (22)$$

for which the particle still may reach the horizon of black string.

In the case of the Schwarzschild spacetime ( $\mathcal{J} = 0$ ) the critical angular momentum reduces to the standard value

$$\mathcal{L}_{\text{cr}(4D)} = \pm 4. \quad (23)$$

One may see from Fig. 2 the increase of critical angular momentum of particles occurs in the presence of nonvanishing parameter  $\mathcal{J}$ . The graph corresponding to the critical angular momentum, which is indicated with the thick line, shifts upwards with the increase of parameter  $\mathcal{J}$ . The presence of parameter  $\mathcal{J}$  causes the particle orbits to become more unstable compared to the case  $\mathcal{J} = 0$ . Bound and escape orbits are forced to become terminated orbits due to the presence of nonvanishing parameter  $\mathcal{J}$ . This effect is shown in more clear way in Fig. 3. The dashed line corresponding to the case  $\mathcal{J} = 0$  is more unstable compared to the case when  $\mathcal{J} = 0$ .

### D. Collision of freely falling particles

In this section we study the collision of two particles near the horizon of the nonrotating black string. Consider two particles approaching the black string with the different angular momenta  $\mathcal{L}_1, \mathcal{J}_1$  and  $\mathcal{L}_2, \mathcal{J}_2$  and colliding at some radius  $r$  at the equatorial plane of the black

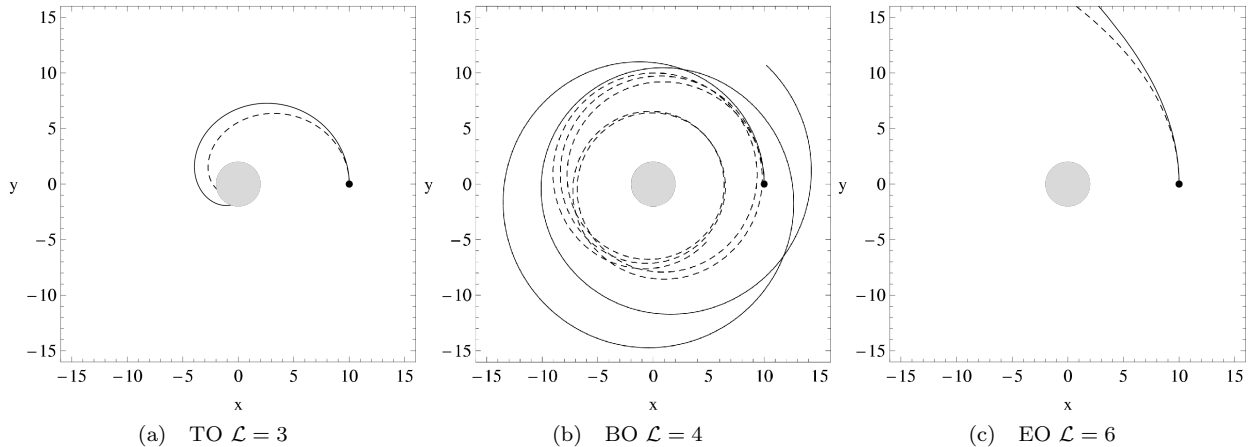


Figure 3: Examples of particle trajectories moving at the equatorial plane around black string. We compare motion with  $\mathcal{J} = 0$  (solid curve) with  $\mathcal{J} = 0.5$  (dashed) for all TO, BO and EO possible orbits. Particles start from the position  $r_0 = 10$  but with the different energies.

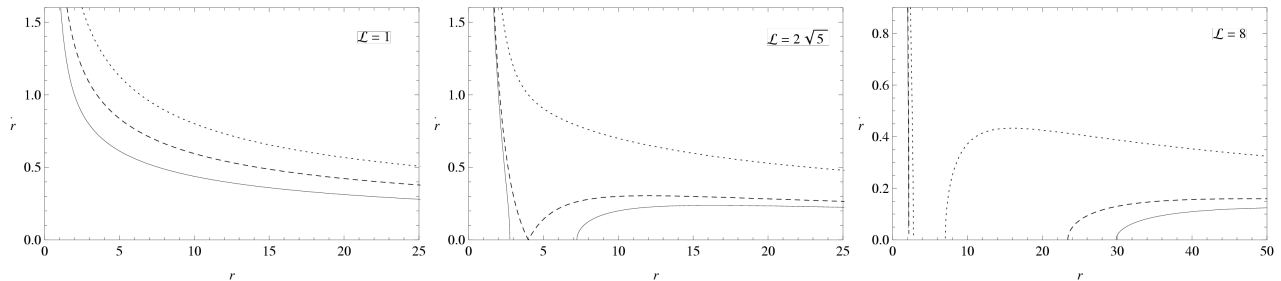


Figure 4: Acceleration of a freely falling particle along the axis  $r$  by the static black string for three different values of parameter  $\mathcal{J}$ :  $\mathcal{J} = 0$  (solid),  $\mathcal{J} = 0.5$  (dashed) and  $\mathcal{J} = 1.5$  (dotted) and three representative values of the angular momentum: left panel corresponds to the case when  $\mathcal{L} = 1$ , middle panel corresponds to the case when  $\mathcal{L} = 4.47$  and right panel corresponds to the case when  $\mathcal{L} = 8$ . The critical case corresponds to the dashed curve in the middle panel.

string. Assume that the particles are at rest at infinity; i.e. their energies satisfy Eq. (20). In the center-of-mass frame the maximal energy will have a place where the particles collide near a black string with maximal and opposite angular momenta given by the expression (22).

Our aim is to compute the energy in the center-of-mass frame for the collision of two particles. Since the background is curved, we need to define the center-of-mass frame properly. It turns out that there is a simple formula for  $E_{c.m.}$  valid both in flat and curved spacetimes:

$$E_{c.m.} = m_0 \sqrt{2} \sqrt{1 - g_{\alpha\beta} U_{(1)}^\alpha U_{(2)}^\beta}, \quad (24)$$

where  $U_{(1)}^\alpha$  and  $U_{(2)}^\beta$  are the five-velocities of the particles, properly normalized by  $g_{\alpha\beta} U^\alpha U^\beta = -1$ . This formula is of course well known in special relativity, and the principle of equivalence should be enough to ensure its validity in a curved background [24]. Components of  $U_{(1)}^\alpha$  and  $U_{(2)}^\beta$  can be straightforwardly calculated from (10) - (13) in the form

$$U_{(1)}^\alpha = \quad (25)$$

$$\left( \frac{(1 + \mathcal{J}_1^2)r}{r - 2}, \pm \frac{\sqrt{2r^3(1 + \mathcal{J}_1^2) - \mathcal{L}_1^2 r(r - 2)}}{r^2}, 0, \frac{\mathcal{L}_1}{r^2}, \mathcal{J}_1 \right),$$

$$U_{(2)}^\alpha = \quad (26)$$

$$\left( \frac{(1 + \mathcal{J}_2^2)r}{r - 2}, \pm \frac{\sqrt{2r^3(1 + \mathcal{J}_2^2) - \mathcal{L}_2^2 r(r - 2)}}{r^2}, 0, \frac{\mathcal{L}_2}{r^2}, \mathcal{J}_2 \right),$$

where the sign ”+” corresponds to incoming particles, while the sign ”-” corresponds to outgoing ones. Here we take the energy of the particle at rest at infinity, i.e.  $\mathcal{E}^2 = 1 + \mathcal{J}^2$ . Thus the energy of two colliding particles with the same mass  $m$  near static black string in the

center-of-mass frame is given by

$$\begin{aligned} \frac{1}{2m^2} E_{\text{c.m.}}^2 &= 1 - \mathcal{J}_1 \mathcal{J}_2 - \frac{\mathcal{L}_1 \mathcal{L}_2}{r^2} + \frac{r \sqrt{1 + \mathcal{J}_1^2} \sqrt{1 + \mathcal{J}_2^2}}{r - 2} \\ &\quad - \frac{\sqrt{2r^2(1 + \mathcal{J}_1^2) - \mathcal{L}_1(r - 2)}}{r^2(r - 2)} \\ &\quad \times \sqrt{2r^2(1 + \mathcal{J}_2^2) - \mathcal{L}_2(r - 2)}. \end{aligned} \quad (27)$$

Ex facte, one can say that Eq. (27) diverges at the singularity  $r = 0$ , the horizon of black string is given by  $r = 2$  and unlimited collisional energy appears in the case of the collision at the horizon. However, it is not satisfied (see Fig. 5) since the numerator of (27) also vanishes at this point. If we observe near the horizon where  $r \rightarrow 2$ , collision of two particles falling on the black string with critical angular momenta given by (22), the energy of the collision will be reduced to the value

$$E_{\text{c.m.}} = m\sqrt{2} \sqrt{1 - \mathcal{J}_1 \mathcal{J}_2 + 9\sqrt{(1 + \mathcal{J}_1^2)(1 + \mathcal{J}_2^2)}}, \quad (28)$$

where  $m$  is the mass of the colliding particles. Evidently the maximal energy of the collision occurs if the values of  $\mathcal{J}_1$  and  $\mathcal{J}_2$  are opposite. In the special symmetric case when the parameters  $\mathcal{J}_{1,2}$  have the same and opposite values:  $\mathcal{J}_1 = -\mathcal{J}_2 = \mathcal{J}$ , the expression (28) for the maximal collision energy per unit mass ( $\mathcal{E}_{\text{c.m.}} = E_{\text{c.m.}}/m$ ) reduces to the following simple form

$$\mathcal{E}_{\text{c.m.}}^{\text{max}} = 4.47\sqrt{1 + \mathcal{J}^2}. \quad (29)$$

In the absence of the additional dimension, i.e. when  $\mathcal{J} = 0$ , the maximal energy of the collision in the center-of-mass frame reduces to  $\mathcal{E}_{\text{c.m.}}^{\text{max}} = 2\sqrt{5}$ , which coincides with the value defined in the Schwarzschild black hole spacetime [24].

It is easy to see from the Fig.6 that the collisional energy infinitely grows when the parameter  $\mathcal{J}$  tends to infinity and formally, one can obtain an arbitrary large energy in such collisions of particles. However, for our purposes this case is not interesting, since the energy of such particles measured at infinity also grows in this limit and the high collision energy is possible only if the initial energy of the particles measured at infinity is also extremely high.

### III. BLACK STRING IMMERSSED IN MAGNETIC FIELD AS ACCELERATOR OF CHARGED PARTICLES

#### A. Dynamical equations

Here we study a charged particle motion in the vicinity of a black string of mass density  $M$  given by the spacetime metric (3) in the presence of an external static axisymmetric and asymptotically uniform magnetic field.

Since the spacetime metric (3) is Ricci flat the commuting Killing vectors  $\xi_{(t)}$  and  $\xi_{(\varphi)}$  satisfy the equations

$$\square \xi^\alpha = 0. \quad (30)$$

These equations coincide with the Maxwell equations  $\square A^\alpha = 0$  for a vector potential  $A^\alpha$  of the electromagnetic field in the Lorentz gauge. In what follows, we use the simplest but realistic case when the magnetic field is considered as a test field in the given gravitational background of the nonrotating black string, in such sense that the magnetic field is homogeneous at the spatial infinity where it has the strength  $B$  [28, 29]. For such configuration of the magnetic field one can easily find the components of the vector potential of the electromagnetic field in the form

$$A^\alpha = \frac{B}{2} \xi_{(\varphi)}^\alpha. \quad (31)$$

Keeping the symmetry hereafter, we assume that  $B \geq 0$ . Finally the five-vector potential  $A_\alpha$  of the electromagnetic field will take a form

$$A_t = A_r = A_\vartheta = A_w = 0, \quad A_\varphi = \frac{1}{2} B r^2 \sin^2 \vartheta. \quad (32)$$

Associated with a timelike  $\xi_{(t)}^\mu$  and spacelike  $\xi_{(\varphi)}^\mu$  and  $\xi_{(w)}^\mu$  Killing vectors one can find the following conserved quantities along a geodesics as

$$\mathcal{E} = \frac{E}{m} = -\xi_{(t)}^\mu \frac{P_\mu}{m} = \left(1 - \frac{2M}{r}\right) \frac{dt}{d\tau}, \quad (33)$$

$$\mathcal{L} = \frac{L}{m} = \xi_{(\varphi)}^\mu \frac{P_\mu}{m} = r^2 \sin^2 \vartheta \left( \frac{d\varphi}{d\tau} + \frac{qB}{2m} \right), \quad (34)$$

$$\mathcal{J} = \frac{J}{m} = \xi_{(w)}^\mu \frac{P_\mu}{m} = \frac{dw}{d\tau}. \quad (35)$$

Here  $P_\mu = mu_\mu + qA_\mu$  is the generalized five-momentum of the particle with mass  $m$  and charge  $q$ . In order to study the charged particle motion in combined gravitational and magnetic fields one can use the Hamilton-Jacobi equation in the following form

$$g^{\mu\nu} \left( \frac{\partial S}{\partial x^\mu} + qA_\mu \right) \left( \frac{\partial S}{\partial x^\nu} + qA_\nu \right) = -m^2, \quad (36)$$

where  $q$  and  $m$  are the charge and mass of the particle, respectively. The Hamiltonian of the charged particle in a magnetic field has the following form

$$2H = g^{\alpha\beta} (p_\alpha + qA_\alpha)(p_\beta + qA_\beta) + m^2, \quad (37)$$

where  $p_\mu = mu_\mu$  is the five momentum of the particle.

Since  $t$ ,  $\varphi$  and  $w$  are the Killing variables one can write the action in the form

$$S = -\mathcal{E}t + \mathcal{L}\varphi + \mathcal{J}w + S_{r\vartheta}(r, \vartheta), \quad (38)$$

where the conserved quantities  $\mathcal{E}$ ,  $\mathcal{L}$  and  $\mathcal{J}$  are the energy, angular momentum and new momentum of a test particle

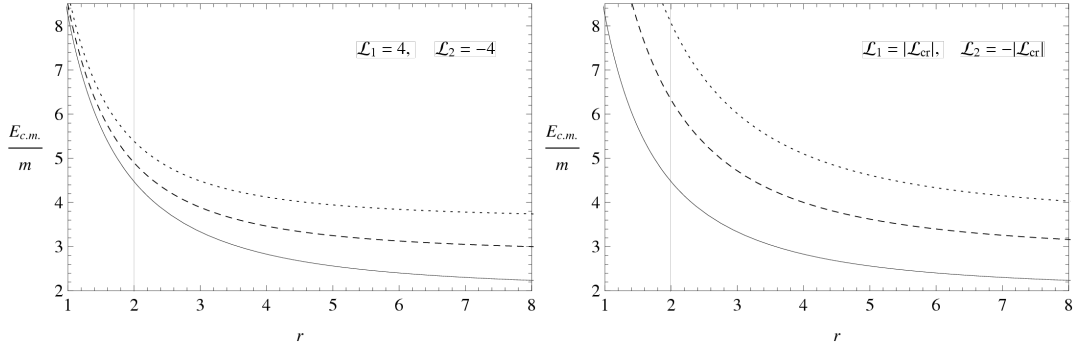


Figure 5: The variation of the energy of the collision of two particles with the opposite momenta near the static black string in the center-of-mass frame for three different values of parameter  $\mathcal{J}$ .  $\mathcal{J}_{1,2} = 0$  (solid),  $\mathcal{J}_{1,2} = \pm 1$  (dashed),  $\mathcal{J}_{1,2} = \pm 1.5$  (dotted). The event horizon is indicated by the vertical thin line.

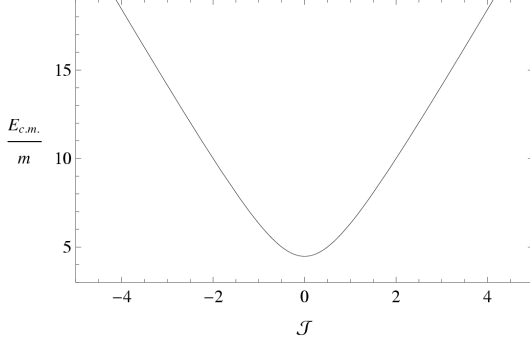


Figure 6: Maximal energy of the collision as function of the parameter  $\mathcal{J}$ .

measured at infinity which is related to the additional dimension. Substituting (38) into Eq. (36) one may get the equation for inseparable part of the action in the form

$$-\left(1 - \frac{2M}{r}\right)^{-1} \mathcal{E}^2 + \left(1 - \frac{2M}{r}\right) \left(\frac{\partial S_{r\vartheta}}{\partial r}\right)^2 + \frac{1}{r^2} \left(\frac{\partial S_{r\vartheta}}{\partial \vartheta}\right)^2 + \frac{1}{r^2 \sin^2 \vartheta} \left(\mathcal{L} + \frac{qB}{2} r^2 \sin^2 \vartheta\right)^2 + \mathcal{J}^2 + m^2 = 0. \quad (39)$$

It is quite easy to separate variables in this equation at the equatorial plane  $\vartheta = \pi/2$  and obtain the differential equations for each coordinate in the following form

$$\frac{dt}{d\tau} = \frac{\mathcal{E}r}{r - 2M}, \quad (40)$$

$$\frac{d\varphi}{d\tau} = \frac{\mathcal{L}}{r^2} - \mathcal{B}, \quad (41)$$

$$\frac{dw}{d\tau} = \mathcal{J}, \quad (42)$$

$$\left(\frac{dr}{d\tau}\right)^2 = \mathcal{E}^2 - V_{\text{eff}}, \quad (43)$$

where the effective potential has a form

$$V_{\text{eff}} = \left(1 - \frac{2M}{r}\right) \left[1 + \mathcal{J}^2 + \left(\frac{\mathcal{L}}{r} - \mathcal{B}r\right)^2\right]. \quad (44)$$

Here we denote new parameter characterizing the coupling between the external magnetic field and the test charged particle as

$$\mathcal{B} = \frac{qB}{2m}. \quad (45)$$

Depending on the direction of the Lorentz force acting on the charged particle the angular momentum of the particle  $\mathcal{L}$  can be either positive or negative. The direction of the Lorentz force does not depend on the parameter  $\mathcal{J}$ , which may, however, change its absolute value. When  $\mathcal{L} > 0$ , the Lorentz force acting on a charged particle is repulsive; i.e., it is directed outward from the black string, and when  $\mathcal{L} < 0$  the Lorentz force is attractive i.e. it is directed towards the black string.

We study the characteristic properties of the motion of charged particles in the exterior spacetime of magnetized black string when  $r > 2M$ . Expression (44) shows that the effective potential is positive in that region and vanishes at the horizon of the black string where  $r = 2M$ . But when  $r \rightarrow \infty$ , the effective potential grows as  $\mathcal{B}^2 r^2$ . This property implies that the particle never reaches the spatial infinity and its motion is always finite. Furthermore, the Lorentz force acting on the charged particle forces the particle to revolve around the axis of the external magnetic field. Due to this it is very important to study the circular motion of the charged particle around black string and especially for the question of the existence of the innermost stable circular orbits.

## B. Circular motion of a charged particle

The minimum of the effective potential corresponds to the circular motion of a particle. Consider a circular motion of a charged particle around a black string. Taking the mass density of the black string as  $M = 1$ , one can write the momentum of a particle at the circular orbit of radius  $r$  as

$$p^\mu = m\gamma \left( \sqrt{\frac{r}{r-2}} \delta_{(t)}^\mu + \frac{v}{r} \delta_{(\varphi)}^\mu + \delta_{(w)}^\mu \right). \quad (46)$$

Here  $v$  (which can be both positive and negative) is a velocity of the particle with respect to a rest frame and

$$\gamma = \frac{1}{\sqrt{1-v^2}} \quad (47)$$

is the Lorentz gamma factor.

Using the expression  $d\varphi/d\tau = v\gamma/r$  together with (34) and (41) one can find

$$v\gamma = \frac{\mathcal{L} - \mathcal{B}r^2}{r}, \quad (48)$$

and easily obtain the expressions for the velocity and the Lorentz gamma factor as

$$v = \frac{\mathcal{L} - \mathcal{B}r^2}{\sqrt{r^2 + (\mathcal{L} - \mathcal{B}r^2)^2}}, \quad (49)$$

$$\gamma^2 = 1 + \left(\frac{\mathcal{L}}{r} - \mathcal{B}r\right)^2. \quad (50)$$

Plots of the velocity and the Lorentz gamma factor at the innermost stable circular orbits (ISCOs) are shown in Fig. 7 for the different values of the parameter  $\mathcal{J}$ . It is obvious from Figs. 7 and 8 that the parameter  $\mathcal{J}$  increases the velocity of the particle and the  $\gamma$  factor is maximal at the end points of the domain of the ISCO radius. The domain of the definition of the ISCO radius is restricted by the region  $2 < r_{\text{ISCO}} < 6$  (see the left panel of Fig. 9). Consequently, the limiting value of the particle velocity at the end of the ISCO domain is

$$v = \sqrt{\frac{1+J^2}{4+J^2}}, \quad (51)$$

which tends to the speed of light ( $v \rightarrow 1 = c$ ) when  $\mathcal{J} \rightarrow \infty$ . Dependence of the velocity of the particle at ISCO on the parameter  $\mathcal{J}$  is presented in Fig. 8. Similarly, the gamma factor of the particle has the maximal value at the end points of the domain of ISCO, namely, at  $r = 2$  and  $r = 6$ . At these positions the gamma factor takes the value

$$\gamma_{\text{max}} = \frac{1}{\sqrt{3}} \sqrt{4+J^2}, \quad (52)$$

which tends to infinity if  $\mathcal{J} \rightarrow \infty$ .

### C. Innermost stable circular orbits

The ISCO is defined by the equations when the first and second derivatives of the effective potential are equal to zero:

$$\mathcal{B}^2 r^4 (r-1) - 2\mathcal{B}\mathcal{L}r^2 + (1+J^2)r^2 - \mathcal{L}^2 r + 3\mathcal{L}^2 = 0, \quad (53)$$

$$\mathcal{B}^2 r^5 + 4\mathcal{B}\mathcal{L}r^2 - 2(1+J^2)r^2 + 3\mathcal{L}^2 r - 12\mathcal{L}^2 = 0. \quad (54)$$

These equations allow one to find the location of the ISCO and parameter  $\mathcal{L}$  for given values of  $\mathcal{B}$  and  $\mathcal{J}$ . Summation of (53) and (54) gives the expression for the angular momentum in terms of  $\mathcal{B}$  and  $r$  as

$$\mathcal{L} = \pm \mathcal{B}r^2 \frac{\sqrt{3r-2}}{\sqrt{6-r}}. \quad (55)$$

Substituting this equation into (54) one can find the interdependency of the magnetic field and ISCO radius for the fixed  $\mathcal{J}$  as follows

$$\mathcal{B} = \frac{\sqrt{(1+J^2)(6-r)}}{r\sqrt{2}\sqrt{2r^2-9r+6 \pm \sqrt{(6-r)(3r-2)}}}. \quad (56)$$

The condition that  $\mathcal{B}$  is real imposes the restrictions on the possible values of the ISCO radius:

$$2 < r_{\text{ISCO}} \leq 6, \quad \text{for } \mathcal{L} > 0, \quad (57)$$

$$\frac{1}{2}(5 + \sqrt{13}) < r_{\text{ISCO}} \leq 6, \quad \text{for } \mathcal{L} < 0. \quad (58)$$

The dependence of the ISCO radii on the magnetic field strength is shown in Fig.9 for two different cases of particle motion:  $\mathcal{L} > 0$  and  $\mathcal{L} < 0$ , when the influence of the Lorentz force on the particle is opposite. One can see from Fig.9, that the magnetic field shifts the ISCO radius towards the horizon of black string. In the limit of the strong magnetic field, i.e., when  $\mathcal{B} \gg 1$ , one can find the value of the ISCO radius for the positive angular momentum as

$$r_{\text{ISCO}} \approx r_{\text{H}} + \frac{\sqrt{1+J^2}}{\sqrt{3\mathcal{B}}}, \quad \mathcal{B} \gg 1, \quad (59)$$

which means that the particle is moving in strong magnetic field and the repulsive Lorentz force has the radius of the innermost stable orbit very close to the horizon of the black string. Recalling that  $\mathcal{B} = qB/2m$ , one can conclude that the ISCO for electrons is located much closer to the horizon than the corresponding orbits for protons. Under the influence of the parameter  $\mathcal{J}$ , the minimal value of the radius of circular orbits increases and charged particles may be shifted towards an observer at infinity which means that the orbits of the charged particles may become unstable.

### D. Collision of particles

In this section, we deviate somewhat from the original idea of BSW [24]. We consider two different situations. In the first case a charged particle orbiting at the ISCO collides with another charged particle at the ISCO. In the second case, we consider the collision of a freely falling from infinity neutral particle with a charged particle revolving at the ISCO instead of a near-horizon collision.



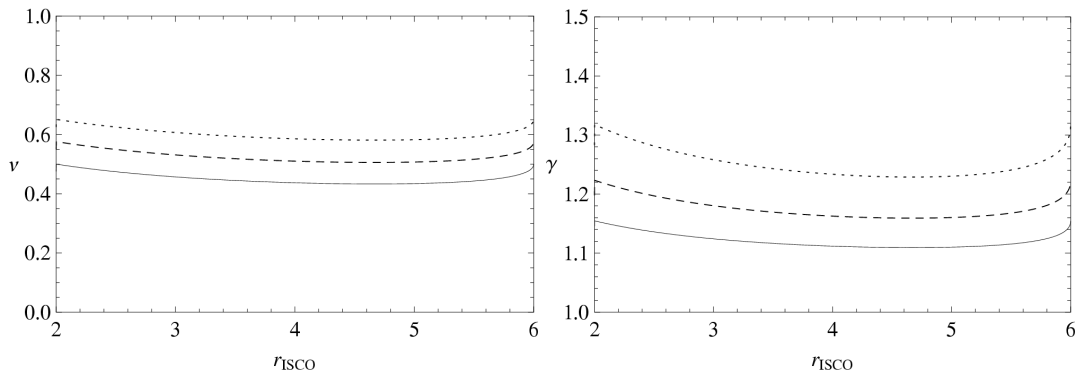


Figure 7: Velocity of the particle and its Lorentz gamma factor at the ISCO as the function of its radius for the positive angular momentum and different values of parameter  $\mathcal{J}$ :  $\mathcal{J} = 0$  (solid),  $\mathcal{J} = 0.7$  (dashed) and  $\mathcal{J} = 1.1$  (dotted).

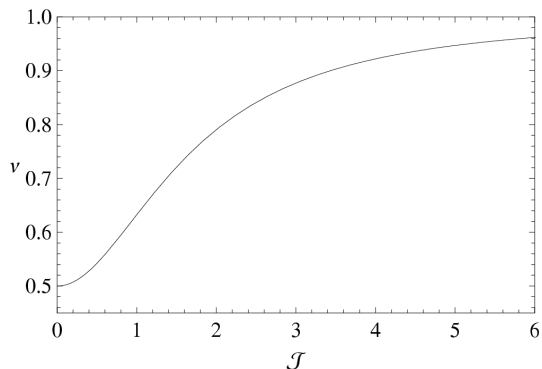


Figure 8: Velocity of the particle at the ISCO as the function of parameter  $\mathcal{J}$ .

### 1. Head-on collision of charged particles orbiting at ISCO

Hereafter, we use the approach and methodology properly developed by Frolov [30]. As a first example we consider a head-on collision of two identical charged particles moving at the same circular orbit in opposite directions with the same mass  $m$ , opposite charges  $+|q|$  and  $-|q|$  and the opposite signs of the parameter  $\mathcal{J}$  and  $-\mathcal{J}$ . The four-momentum of the system after the collision is  $P^\mu = 2m\gamma(1 - 2/r)^{-1/2}\xi_{(t)}^\mu$ . Then the energy after the collision calculated in the center-of-mass frame  $E_{c.m.}$  has the following form [30]:

$$E_{c.m.} = 2m\gamma. \quad (60)$$

For the particle orbiting at the ISCO around a static black string with the fixed parameter  $\mathcal{J}$ , the gamma factor remains almost unchanged along the range of the ISCO for any value of the strength of the magnetic field (see Fig. 7). A substitution of the maximal value of the gamma factor given by Eq. (52) into (60) gives the equation for the maximal center-of-mass energy per unit mass ( $\mathcal{E}_{c.m.} = E_{c.m.}/m$ ) in the form

$$\mathcal{E}_{c.m.}^{\max} = 1.15\sqrt{4 + \mathcal{J}^2}. \quad (61)$$

For the minor values of the parameter  $\mathcal{J}$ , the energy of the collision is slightly higher than  $2m$ . However, similarly to the case of the absence of the magnetic field given by Eq.(29) it is easy to see that the energy of the collision of two particles initially revolving at the ISCO infinitely grows when the parameter  $\mathcal{J}$  tends to infinity and formally one can obtain an arbitrary large energy. However, it does not provide the colliding particles with high energy since the energy of such particles as measured at infinity also grows in this limit.

### 2. Collision of a freely falling neutral particle with a charged particle at ISCO

Now we consider the collision of two particles when one of them is charged and revolved at the ISCO and the other one is neutral and freely falls from infinity in the direction of the black string horizon. We assume that both particles move at the equatorial plane  $\vartheta = \pi/2$  of the black string. In the center-of-mass frame the maximal energy would have place when the particles collide near a black string with maximal and opposite angular momenta. For a neutral particle this condition is defined by the expression (22). At the moment of the collision, the momentum is the sum

$$P^\alpha = p_c^\alpha + p_n^\alpha, \quad (62)$$

where  $p_c^\alpha$  and  $p_n^\alpha$  are momenta of charged and neutral particles, respectively. This corresponds to the collisional center-of-mass energy which can be written in the form

$$E_{c.m.}^2 = m_c^2 + m_n^2 - 2g_{\mu\nu}p_c^\mu p_n^\nu. \quad (63)$$

Using the equations (10)-(13) and (46) one can find the center-of-mass energy of the collision as

$$E_{c.m.}^2 = m_c^2 + m_n^2 + 2m_c\gamma_c \left( \mathcal{E}_n \sqrt{\frac{r}{r-2}} - \frac{v_c \mathcal{L}_n}{r} - \mathcal{J}_n \right), \quad (64)$$

where subscript  $n(c)$  is responsible for neutral(charged) particles. Since the radius of the ISCO can be arbitrarily close to the horizon, the first term in the brackets

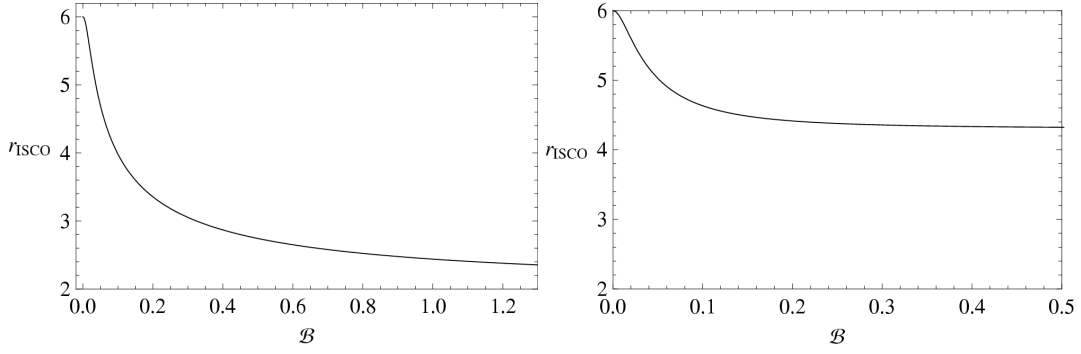


Figure 9: Dependence of the innermost stable circular orbits  $r_{\text{ISCO}}$  on the magnetic field parameter  $\mathcal{B}$ . The left panel corresponds to the motion of the particle with positive angular momentum while right panel corresponds to the particle with negative angular momentum  $\mathcal{L}$ .

can be made arbitrarily large while  $\gamma$  remains finite (see Fig.7 (b)). The second and the third terms in the brackets are finite for the typical values of the parameter  $\mathcal{J}$  (see Eq.(22) and Fig.7 (a)). Consequently, the leading contribution to the energy of the collision near the horizon can be written in the following form:

$$E_{\text{c.m.}}^2 \approx \frac{2\sqrt{2}m_c\gamma_c\mathcal{E}_n}{\sqrt{r-2}} \quad (r \rightarrow 2). \quad (65)$$

Using the relation (59), one can obtain the asymptotic value of the center-of-mass energy for a collision of a neutral particle with the charged one at ISCO in a magnetic field  $\mathcal{B} \gg 1$  as

$$E_{\text{c.m.}}^2 \approx 2\sqrt{2}m_c\gamma_c\mathcal{E}_n \left( \frac{\sqrt{3}\mathcal{B}}{\sqrt{1+\mathcal{J}^2}} \right)^{1/2}. \quad (66)$$

Using Eqs. (50), (55), and (56) at the horizon  $r = 2$  and assuming that the neutral particle starts its motion at the rest at infinity with the energy given by (20) as  $\mathcal{E}_n = \sqrt{1+\mathcal{J}^2}$ , one can obtain the collisional energy per unit mass ( $\mathcal{E}_{\text{c.m.}} = E_{\text{c.m.}}/m$ ) in the following form:

$$\mathcal{E}_{\text{c.m.}}^{\text{max}} \approx 1.74 \left( \mathcal{B}\sqrt{1+\mathcal{J}^2} \right)^{1/4}. \quad (67)$$

#### IV. ROTATING BLACK STRING AS PARTICLE ACCELERATOR

##### A. Dynamical equations

As it is generally known, the metric of the Kerr black hole spacetime is the four-dimensional rotating neutral axially symmetric solution of the vacuum Einstein equations. When the additional dimension  $w$  is included to the metric of the Kerr spacetime in the Boyer-Lindquist coordinates then the obtained solution takes the follow-

ing form [2, 3]

$$ds^2 = \frac{\rho^2}{\Delta_r} dr^2 + \rho^2 d\vartheta^2 + dw^2 - \frac{\Delta_r}{\rho^2} (dt - a \sin^2 \vartheta d\varphi)^2 + \frac{\sin^2 \vartheta}{\rho^2} [(r^2 + a^2)d\varphi - a dt]^2, \quad (68)$$

where the metric parameters  $\Delta_r$  and  $\rho$  are defined as

$$\Delta_r = r^2 - 2Mr + a^2, \quad \rho^2 = r^2 + a^2 \cos^2 \vartheta. \quad (69)$$

Eq. (68) is the metric of the spacetime of a uniform rotating black string. Here  $M$  is the mass density of the black string and  $a$  is the parameter of the rotation of the black string with the relation  $0 \leq a/M \leq 1$ . The singularity, as usually, placed at  $\rho^2 = 0$ , (or at  $r = 0$  and  $\vartheta = \pi/2$ ). This implies, that as in the Kerr geometry, the motion of a particle along the geodesic line with  $r = 0$  and  $\vartheta \neq \pi/2$  will not end at the point of singularity, and the negative values of  $r$  are allowed in the rotating black string spacetime. [3, 47]. The expression  $\Delta_r = 0$ , allow us to define the event horizons of the black string as

$$r_{\pm} = M \pm \sqrt{M^2 - a^2}, \quad (70)$$

which coincide with the event horizon in the Kerr spacetime.

Associated with a timelike  $\xi_{(t)}^\mu$  and spacelike  $\xi_{(\varphi)}^\mu$  and  $\xi_{(w)}^\mu$  Killing vectors one can find the following conserved quantities along a geodesic line on the equatorial plane  $\vartheta = \pi/2$  as:

$$\mathcal{E} = \frac{E}{m} = -\xi_{(t)}^\mu u_\mu = \left( 1 - \frac{2M}{r} \right) \frac{dt}{d\tau} + \frac{2Ma}{r} \frac{d\varphi}{d\tau}, \quad (71)$$

$$\mathcal{L} = \frac{L}{m} = \xi_{(\varphi)}^\mu u_\mu = \left( r^2 + a^2 + \frac{2Ma^2}{r} \right) \frac{d\varphi}{d\tau} - \frac{2Ma}{r} \frac{dt}{d\tau}, \quad (72)$$

$$\mathcal{J} = \frac{J}{m} = \xi_{(w)}^\mu u_w = \frac{dw}{d\tau}. \quad (73)$$

The Hamilton-Jacobi equation (4) can be separated and gives a differential equation for each component as

[3]

$$\frac{dt}{d\tau} = \frac{1}{\Delta r} [\mathcal{E}(r^3 + 2Ma^2 + a^2r) - 2aM\mathcal{L}], \quad (74)$$

$$\frac{d\varphi}{d\tau} = \frac{1}{r\Delta} [2aM\mathcal{E} + (r-2)\mathcal{L}], \quad (75)$$

$$\frac{dw}{d\tau} = \mathcal{J}, \quad (76)$$

$$\left(\frac{dr}{d\tau}\right)^2 = \mathcal{E}^2 - V_{\text{eff}}, \quad (77)$$

where the effective potential has a form

$$V_{\text{eff}} = \frac{1}{r^2} \left[ \mathcal{L}^2 \left( 1 - \frac{2M}{r} \right) - a^2 \mathcal{E}^2 \left( 1 + \frac{2M}{r} \right) + 2a\mathcal{E}\mathcal{L} \frac{2M}{r} + \Delta (1 + \mathcal{J}^2) \right]. \quad (78)$$

For getting the solutions of the equations of motion outside the event horizon one has to hold the condition  $dt/d\tau > 0$ . At the region close to the horizon  $r \rightarrow r_+$ , this condition gives the limiting value of the angular momentum of the particle as

$$\mathcal{L} \leq \mathcal{L}_H = \frac{2\mathcal{E}}{a} \left( 1 + \sqrt{1 - a^2} \right). \quad (79)$$

Equation (79) is similar for both Kerr black hole and rotating black string spacetimes. However, for the particle falling on the horizon with the initial rest energy (20), the limiting (maximal) value of the angular momentum takes the form

$$\mathcal{L}_H = \frac{2}{a} \left( 1 + \sqrt{1 - a^2} \right) \sqrt{1 + \mathcal{J}^2}. \quad (80)$$

The variation of the function  $\mathcal{L}_H$  with dependence on the spin parameter  $a$  for the different values of the parameter  $\mathcal{J}$  is shown in Fig.10. It is easy to see that when the value of the parameter  $\mathcal{J}$  increases, the limiting allowed value of the angular momentum also increases. Samples of particle trajectories moving in equatorial plane around rotating black string are shown in Fig. 11 for the different values of parameter  $\mathcal{J}$  when the spin parameter  $a = 0.99$ , depicting the change from TO to BO and EO orbits. Such transitions is shown in Fig.12 for  $a = 0$  and  $a = 0.99$ .

### B. Freely falling particle

In this subsection, we study the properties of the freely falling particles into the rotating black string and approaching the horizon with the different values of momenta  $\mathcal{L}_1$ ,  $\mathcal{J}_1$  and  $\mathcal{L}_2$ ,  $\mathcal{J}_2$  at the equatorial plane  $\vartheta = \pi/2$  of the black string.

It is very important to find the limitations on the possible values of the integrals of motion  $\mathcal{L}$  and  $\mathcal{J}$  of particles to achieve the horizon of the rotating black string as we

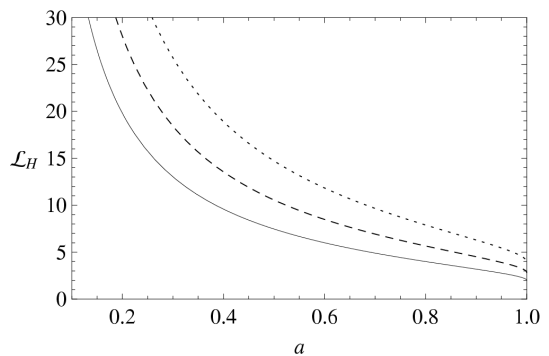


Figure 10: The limiting value of the angular momentum of the particle near the horizon  $r = r_+$  of the rotating black string with dependence on the spin parameter  $a$  for the different values of the parameter  $\mathcal{J}$ :  $J = 0$  (solid),  $J = 1$  (dashed),  $J = 1.7$  (dotted). The area of the possible values of the angular momentum is shaded.

did in Sec.II C. In the center-of-mass frame the maximal energy will take place when the particles collide near a rotating black string with maximal and opposite momenta  $\mathcal{L}_1$ ,  $\mathcal{L}_2$  and parameters  $\mathcal{J}_1$ ,  $\mathcal{J}_2$ . But if we set the large values for them, then the geodesics may never reach the vicinity of the horizon (see the plots with  $\mathcal{L} = 1.6$  in Fig. 13) and effects of the strong gravitational field cannot be analyzed. On the other hand, for the small values of angular momentum, the particles fall radially with a small tangential velocity and the center-of-mass energy does not grow either (see the plots with  $\mathcal{L} = 2.6$  in Fig. 13). In spacetime of rotating black string, the particles approaching from one side or the other have different properties which are similar to their properties in Kerr spacetime. Consequently, there are critical values for the parameters  $\mathcal{L}$  and  $\mathcal{J}$  such that particles may reach the horizon with maximum tangential velocity (see thick curves in Fig. 13). To find these values we use Eq. (77) and its derivative. The profiles of the variation of  $\dot{r}$  with radius for the different values of the parameters  $\mathcal{J}$  and  $\mathcal{L}$  are shown in Fig.14, where the critical case when the particle approaches the horizon of the black string is indicated by the dashed curve of the plot (b).

In order for the massive particle freely falling with momentum  $\mathcal{J}$  to the black string with the spin parameter  $a$  to achieve the horizon, it must have the angular momentum in the range

$$\mathcal{L}_- \leq \mathcal{L} \leq \mathcal{L}_+, \quad (81)$$

where  $\mathcal{L}_+$  and  $\mathcal{L}_-$  are defined as

$$\mathcal{L}_+ = 2\sqrt{1 + \mathcal{J}^2} (1 + \sqrt{1 - a}), \quad (82)$$

$$\mathcal{L}_- = -2\sqrt{1 + \mathcal{J}^2} (1 + \sqrt{1 + a}). \quad (83)$$

It is important to note that this does not apply when the particle scatters with other particles and changes its

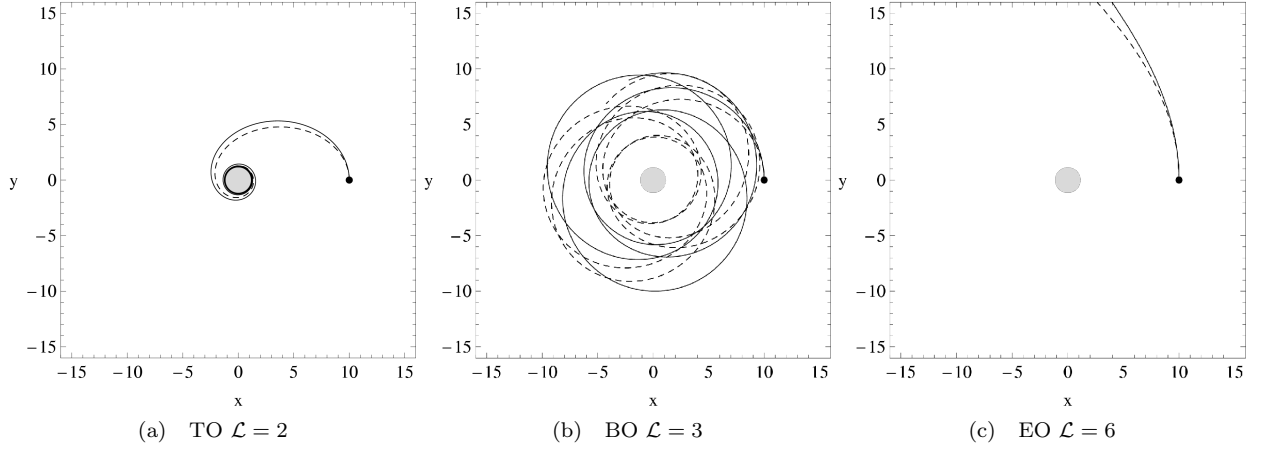


Figure 11: Examples of particle trajectories moving in equatorial plane around rotating black string when the spin parameter  $a = 0.99$ . We compare motion with  $\mathcal{J} = 0$  (solid curve) and with  $\mathcal{J} = 0.5$  (dashed) for all TO, BO and EO possible orbits. Particles start from the initial position  $r_0 = 10$  but with the different energies.

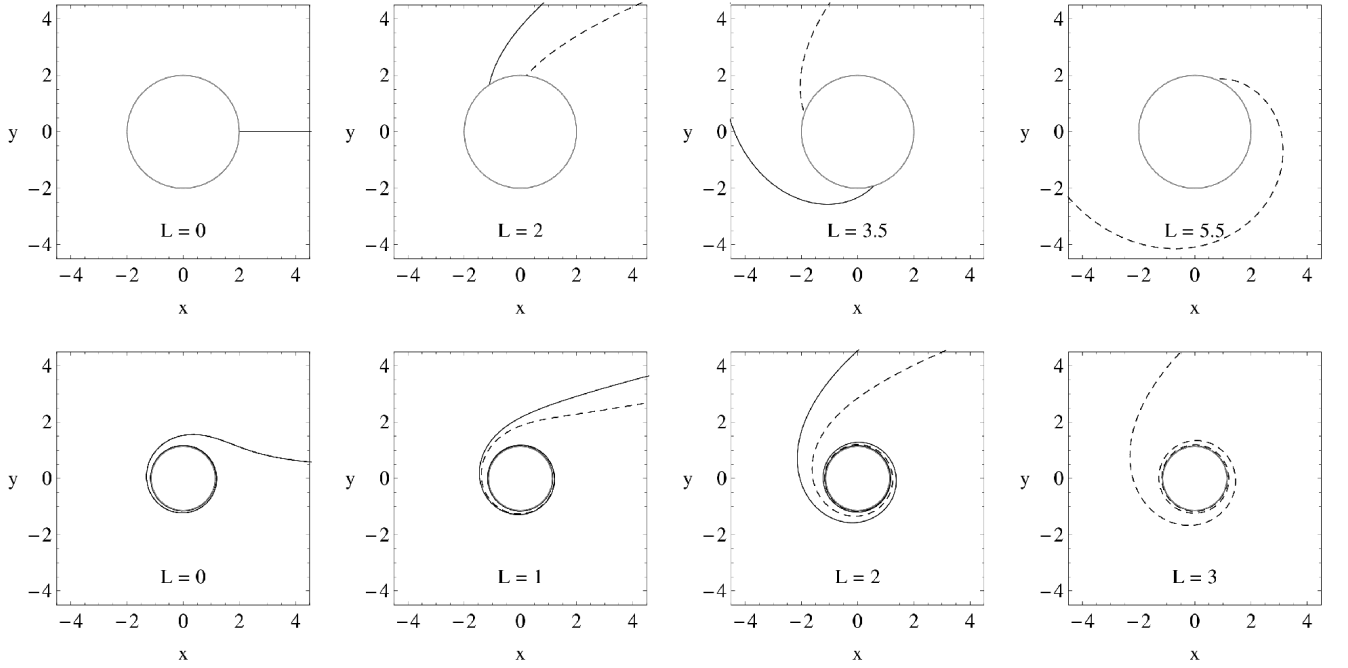


Figure 12: We compare TO for particle motion with  $\mathcal{J} = 0$  (solid curve) and with  $\mathcal{J} = 1$  (dashed one), depicting dependence of "ending angle"  $\varphi_{\text{end}}$  from the specific angular momenta  $\mathcal{L}$  for the case when the spin parameter is  $a = 0$  and  $a = 0.99$ . Particles start from the "infinity" (at  $r_0 = 1000$ ) with energies  $E \doteq 1$  (for  $\mathcal{J} = 0$ ) and  $\mathcal{E} \doteq 1.4$  (for  $\mathcal{J} = 1$ ). For some critical values of angular momenta  $\mathcal{L}$  the TO orbits become BO and hence are not visible on the graphs. Such critical value  $\mathcal{L}_c$  is growing with parameter  $\mathcal{J}$  (For the case when  $a = 0$  we have  $\mathcal{L}_c = 4\sqrt{1 + \mathcal{J}^2}$ ). We also see strong "winding" of particle trajectories onto event horizon of black string when  $a = 0.99$ . Even orbits with  $\mathcal{L} = 0$  have nonzero "ending angle"  $\varphi_{\text{end}}$ .

energy and angular momentum on the way to the horizon. The dependence of the critical angular momenta  $\mathcal{L}_{\pm}$  of the particle reaching the horizon of the extremal black string on the values of parameter  $\mathcal{J}$  are shown in Fig.15. It can be seen that the solutions of the equation for the particle moving in the spacetime of black string are invariant under the reversal of sign of parameter  $\mathcal{J}$ .

When the extra dimension is added, the absolute values of the critical angular momenta increase for any value of the spin parameter  $a$ .

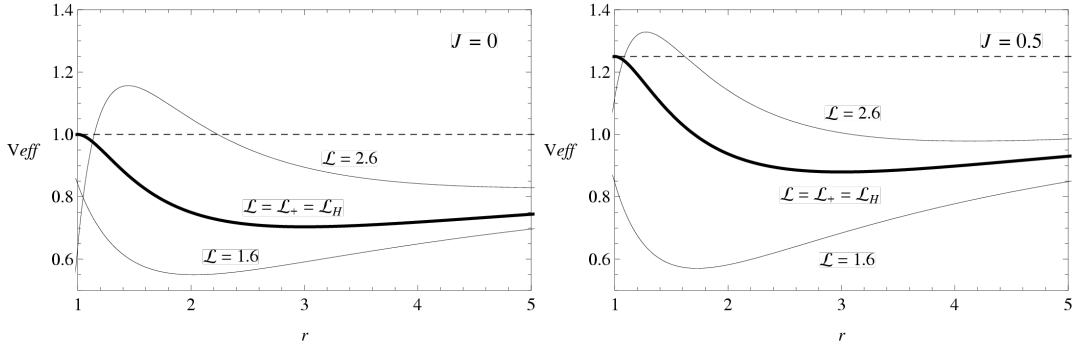


Figure 13: The radial dependence of the effective potential of the particle moving around extremally rotating black string with  $a = 1$  for the different values of the angular momentum  $\mathcal{L}$  in two different cases of the absence (left panel) and presence (right panel) of the parameter  $J$ . Dashed lines indicate the energy level of a free particle at infinity.

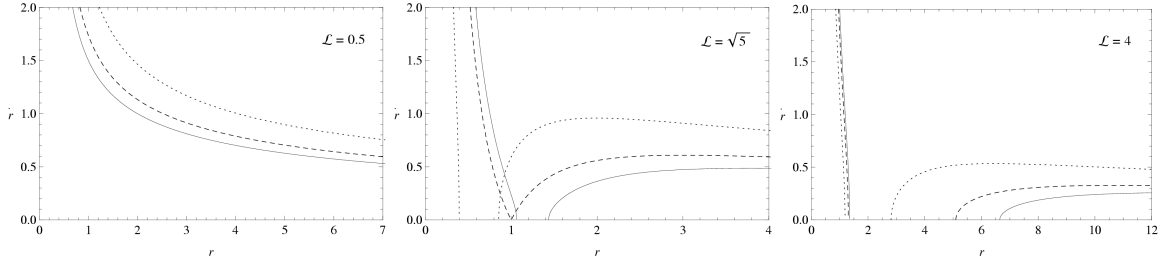


Figure 14: Acceleration of particle along  $r$  by extremally rotating black string for three different values of the parameter  $\mathcal{J}$ :  $\mathcal{J} = 0$  (solid),  $\mathcal{J} = 0.5$  (dashed) and  $\mathcal{J} = 1$  (dotted) and three different values of the angular momentum:  $\mathcal{L} = 0.5$  (left panel),  $\mathcal{L} \approx 2.24$  (middle panel) and  $\mathcal{L} = 4$  (right panel). Critical case corresponds to the dashed curve in the middle panel.

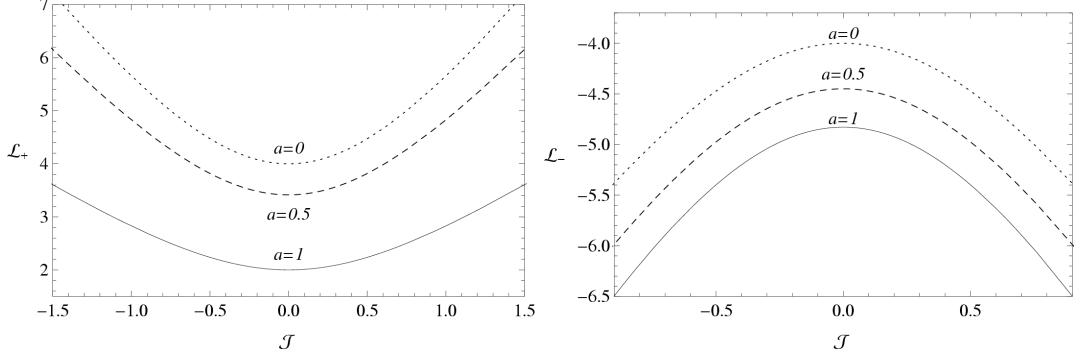


Figure 15: Dependence of the critical angular momentum  $\mathcal{L}_{\pm}$  of the particle on the parameter  $\mathcal{J}$  for the different values of the spin parameter  $a$  of the black string.

### C. Collision of freely falling particles near extremally rotating black string

In this subsection we study the collision of two particles approaching the horizon of the extremally rotating black string with the different momenta  $\mathcal{L}_1$ ,  $\mathcal{J}_1$  and  $\mathcal{L}_2$ ,  $\mathcal{J}_2$  at the equatorial plane  $\vartheta = \pi/2$  of the black string.

First, we derive the general formula for the center-of-mass energy of the collision of two particles freely falling from the spatial infinity to the horizon of the rotating black string. Considering the center-of-mass frame and a pair of particles with the same mass  $m_0$  and velocities

represented by  $U_{(m)} = U_{(m)}^{\mu}$ , one can write the expression for the energy of the collision of two particles in the form

$$E_{c.m.}^2 = \left( mU_{(1)}^{\alpha} + mU_{(2)}^{\alpha} \right) \left( mU_{(1)\alpha} + mU_{(2)\alpha} \right) = 2m^2 \left( 1 + U_{(1)}^{\alpha} U_{(2)\alpha} \right), \quad (84)$$

or in the form similar to (24) as

$$E_{c.m.} = m_0 \sqrt{2} \sqrt{1 - g_{\alpha\beta} U_{(1)}^{\alpha} U_{(2)}^{\beta}}, \quad (85)$$

where  $U_{(1)}^{\alpha}$  and  $U_{(2)}^{\beta}$  are the velocities of the particles,

properly normalized by  $g_{\alpha\beta}U^\alpha U^\beta = -1$ . Direct substitution of Eqs. (74) - (77) to (85) gives the expression for the energy of the collision of two particles ( $\mathcal{E}_{c.m.} = E_{c.m.}/m_0$ )

$$\mathcal{E}_{c.m.}^2 = \frac{2}{r\Delta} \left\{ a^2 [\mathcal{E}_1 \mathcal{E}_2 (2+r) + r(1 - \mathcal{J}_1 \mathcal{J}_2)] - 2a(\mathcal{E}_2 \mathcal{L}_1 + \mathcal{E}_1 \mathcal{L}_2) + r^2 [(1 - \mathcal{J}_1 \mathcal{J}_2)(r-2) + \mathcal{E}_1 \mathcal{E}_2 r] - \mathcal{L}_1 \mathcal{L}_2 (-2+r) - \sqrt{R_1} \sqrt{R_2} \right\}, \quad (86)$$

colliding at some radius  $r$  at the equatorial plane which is the generalization of Eq.(27) to the case of the rotating black string spacetime.

Here

$$R_i = 2(a\mathcal{E}_i - \mathcal{L}_i)^2 - \mathcal{L}_i^2 r + 2r^2 \mathcal{L}_i^2, \quad i = 1, 2, \quad (87)$$

and

$$\mathcal{E}_i = \sqrt{1 + \mathcal{J}_i^2} \quad i = 1, 2 \quad (88)$$

for the freely falling particles.

Ex facte, one can say that Eq. (86) diverges at the horizon of the black string given by  $\Delta = 0$  and extremal collisional energy appears. However, it is not satisfied (see Fig. 16) since the numerator of Eq. (86) also vanishes at this point. This result corresponds to the result of the paper [24] in the case when  $\mathcal{J}_i = 0$ .

To find a limit of the energy at the horizon  $r \rightarrow r_+$  one may use the l'Hospital's rule and find the actual extremal collisional energy at the horizon of extremely rotating black string with  $a = 1$ . Thus, the energy of the collision in the special case with  $\mathcal{J}_1 = -\mathcal{J}_2 = \mathcal{J}$  (which is relevant due to the symmetry of the additional dimension) will have the following form

$$\mathcal{E}_{c.m.}^2|_{(r \rightarrow r_+)} = 2(1 + \mathcal{J}^2) \times \left( \frac{\mathcal{L}_1 - 2\sqrt{1 + \mathcal{J}^2}}{\mathcal{L}_2 - 2\sqrt{1 + \mathcal{J}^2}} + \frac{\mathcal{L}_2 - 2\sqrt{1 + \mathcal{J}^2}}{\mathcal{L}_1 - 2\sqrt{1 + \mathcal{J}^2}} \right). \quad (89)$$

Expression (89) diverges when the dimensionless angular momentum of one of the colliding particles  $\mathcal{L} = \mathcal{L}_+$  and on the contrary finite for the generic values of  $\mathcal{L}_1$  and  $\mathcal{L}_2$ . Thus for extremely rotating black strings the scattering energy in the center-of-mass frame becomes unlimited when  $\mathcal{L} = \mathcal{L}_+$ .

This shows that a singularity in the center-of-mass energy is achieved on the extremal horizon for most specific values of angular momentum and is finite for the generic values of momentum  $\mathcal{L}$ . In this case, every value of the finite energy is achieved up to the event horizon and infinite center-of-mass energy is obtained only for particle collisions occurring on the horizon as shown in Ref. [24]. If the angular momentum of both individual particles is greater than the critical one, then they will never reach the horizon. Vice versa, if they both have angular momentum below the critical value, then they will fall into the black string with a finite center-of-mass collisional energy.

## D. The collision energy near nonextremely rotating black string

It has been recently shown in Ref.[48] that an arbitrarily high energy of the collision of two freely falling particles near a Kerr black hole cannot occur if a spin parameter  $a$  is not maximal. Similarly, in the spacetime of a rotating black string as we will show below, there is no possibility to obtain an unlimited energy from the collision of freely falling from infinity particles if the rotation of the black string is not extremal. However, in the processes accompanied by the multiple scattering when the particles fall into the black string and collide with other particles moving around a horizon of the black string high energy collision can be obtained even if the rotation of the black string is not maximal, i.e.,  $a < 1$ . In this subsection we study the possibility of the extraction of the unlimited energy from the particles collision for the case of a nonextremal black string.

As mentioned above, Eq. (77) leads to an appearance of the limitation on the possible values of the angular momenta of freely falling particles to reach the horizon of the black string. For the rotating black string, this condition is given by Eq.(81). Using the limiting values of the angular momenta (82) and (83) of the particles at the horizon of the rotating black string one can find the dependence of the center-of-mass energy on the spin parameter  $a$  which is shown in Fig.17. It can be seen from Fig.17 that the unlimited energy occurs when the black string rotates with the maximal spin parameter  $a = 1$ , while for a black string with spin parameter  $a < 1$ , there will be an upper bound to the energy. It is very interesting to find how the largest energy of the collision grows as the maximally spinning case is approached. The maximal energy can be estimated with the help of Eq.(86). In terms of the small parameter  $\epsilon = 1 - a$ , the main contribution to the energy of the collision per unit mass is

$$\mathcal{E}_{c.m.}^{\max} \approx \frac{4.06}{\sqrt[4]{\epsilon}} [(1 + \mathcal{J}_1^2)(1 + \mathcal{J}_2^2)]^{1/4}. \quad (90)$$

In particular, according to [50] the maximal possible value of the spin parameter  $a$  of the astrophysical black holes is  $a = 0.998$ . If one applies this limiting value of the spin parameter for the estimation of the collision energy of two particles with  $\mathcal{J}_1 = \mathcal{J} = -\mathcal{J}_2$  near the horizon of the rotating black string, then the maximal possible center-of-mass energy takes the value

$$\mathcal{E}_{c.m.}^{\max} = 18.971 \sqrt{1 + \mathcal{J}^2}, \quad a = 0.998. \quad (91)$$

It can be seen that even for the values of the spin parameter  $a$  being close to the extremal  $a = 1$  of the rotating black string energy,  $E_{c.m.}/m$  cannot be unlimited. However, as it has been already noted in Sec.II the expression (91) for the collisional energy tends to infinity if the parameter  $\mathcal{J}$  also grows in this limit ( $\mathcal{J} \rightarrow \infty$ ) and formally one can obtain an arbitrarily large energy. However this

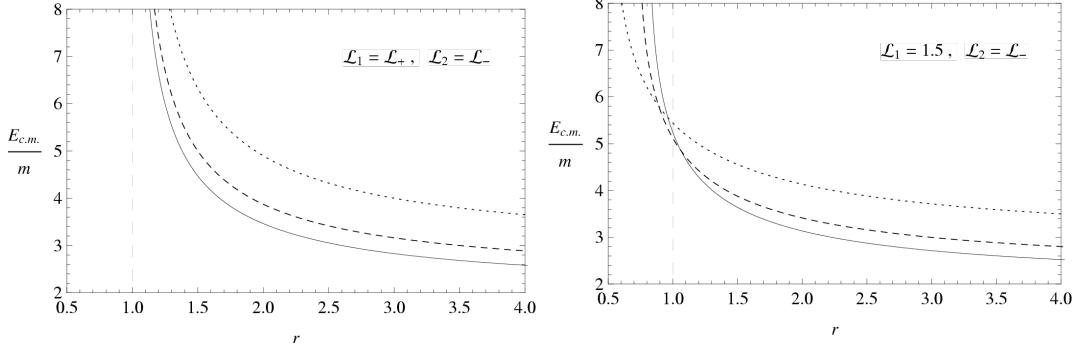


Figure 16: The variation of the energy of the collision of two particles with opposite momenta near the static black string in the center-of-mass frame for three different values of parameter  $\mathcal{J}$ .  $\mathcal{J}_{1,2} = 0$  (solid),  $\mathcal{J}_{1,2} = \pm 1$  (dashed),  $\mathcal{J}_{1,2} = \pm 1.5$  (dotted). The event horizon is indicated by vertical thin line.

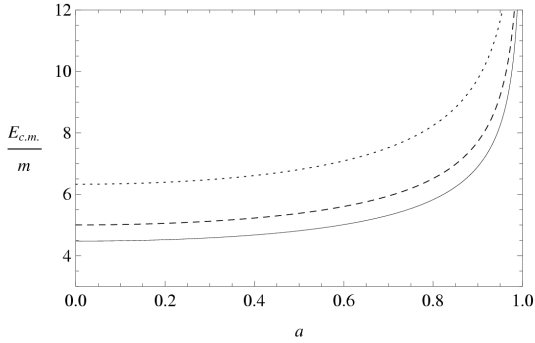


Figure 17: The center-of-mass energy of the collision of two freely falling particles close to the horizon of the rotating black string in dependence on the spin parameter  $a$  for three representative values of the parameter  $\mathcal{J}_{1,2}$  of each particle:  $\mathcal{J}_{1,2} = 0$  (solid),  $\mathcal{J}_{1,2} = \pm 0.5$  (dashed), and  $\mathcal{J}_{1,2} = \pm 1$  (dotted).

case does not correspond to our purposes since this high energy is not the result of the collision of particles near the horizon of the rotating black string but the result of an enormous increase of the initial energies of the particles measured at infinity.

On the other hand, one may take into account the possibility of a multiple scattering of the particle falling from infinity with the fixed angular momentum. As the result of interaction with the particles from the accreting disc, the particle falling into the black string can change its momentum and again scatter close to the horizon, and finally the scattering energy can be unlimited [49].

A particle moving from infinity to the black string can achieve the horizon if its angular momentum is lying in the range  $\mathcal{L}_- \leq \mathcal{L} \leq \mathcal{L}_+$  (see the dependence of  $\mathcal{L}_-$  and  $\mathcal{L}_+$  from  $\mathcal{J}$  in Fig. 15). The effective potential of the particle in the spacetime of nonextremely rotating black string for the different values of  $\mathcal{L}$  and  $\mathcal{J}$  is shown in Fig. 18. The particle can move in the vicinity of the black string if its energy  $\mathcal{E} < \sqrt{1 + \mathcal{J}^2}$ . Zones of allowed particle motion in the horizon vicinity are shaded in Fig. 18.

One can see from Fig. 18 that the presence of the new constant of motion  $\mathcal{J}$  shifts and increases the allowed zone of particle motion. However, if the particle is going not from the infinity but from a distance  $r = r_H + e$  then due to the form of the effective potential it may have the angular momentum of the value  $\mathcal{L} = \mathcal{L}_H - \delta$  larger than  $\mathcal{L}_+$  and fall on the horizon. On the other hand if the particle falling from infinity with  $\mathcal{L} \leq \mathcal{L}_+$  achieves the same region  $r = r_H + e$  and interacts with other particles of the accretion disc or decays into a lighter particle which results in an increased angular momentum  $\mathcal{L}_1 = \mathcal{L}_H - \delta$ , then the main contribution to the scattering energy in the center-of-mass frame according to Eq. (86) takes the form

$$\mathcal{E}_{c.m.} \approx \frac{\sqrt{2}}{\sqrt{\delta}} \left( \frac{\mathcal{L}_H - \sqrt{1 + \mathcal{J}^2} \mathcal{L}_2}{1 - \sqrt{1 - a^2}} \right)^{\frac{1}{2}} (1 + \mathcal{J}^2)^{\frac{1}{4}}, \quad (92)$$

if expanded in series.

For the rotation parameter  $a = 0.998$  and  $\mathcal{L}_2 = \mathcal{L}_-$ , the expression (92) reduces to the form

$$\mathcal{E}_{c.m.}^{\max} = \frac{3.854}{\sqrt{\delta}} (1 + \mathcal{J}^2)^{3/4}. \quad (93)$$

The energy (92) grows without limit when  $\delta \rightarrow 0$ . Note that for rapidly rotating black strings, the difference between  $\mathcal{L}_H$  and  $\mathcal{L}_+$ , e.g., for  $a = 0.998$  and  $\mathcal{J} = 0.7$ ,  $\mathcal{L}_H - \mathcal{L}_+ \approx 0.05$ . The possibility of getting small additional angular momentum in interaction close to the horizon seems to be very probable.

## V. EFFICIENCY OF ENERGY EXTRACTION

Consider the geodesics of the particles in the equatorial plane  $\vartheta = \pi/2$ . The radial equation of motion in the spacetime metric (3) is given by

$$\frac{m^2}{2} \left( \frac{dr}{d\tau} \right)^2 + V(r) = 0, \quad (94)$$

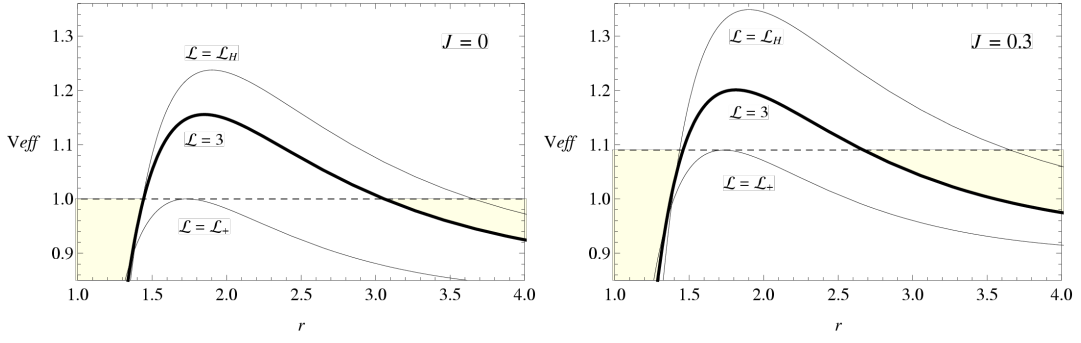


Figure 18: The effective potential of the particle moving around nonextremal black string with  $a = 0.9$  in the absence (left panel) and the presence (right panel) of the parameter  $\mathcal{J}$ . The allowed zone for  $\mathcal{L} = 2.5$  is shaded. Dashed lines represent the energy level of a free particle at infinity.

where  $m$  is the mass,  $E$  is the energy,  $L$  is the momentum of the particle, and

$$V(r) = \frac{\Delta}{2r^2}(m^2 + J^2) + \frac{L^2 - a^2 E^2}{2r^2} - \frac{M(L - aE)^2}{r^3} - \frac{E^2}{2} \quad (95)$$

is the effective potential of radial motion of the particle.

Consider the particle escape to infinity analysing the effective potential (95). Using the condition  $V(r) = 0$  one can obtain

$$b = b_{\pm}(r) = \frac{-2aM \pm r\sqrt{\Delta(1 - \kappa(1 - 2M/r))}}{r - 2M}, \quad (96)$$

for the the impact parameter  $b = L/E$  for the massless particle, where new dimensionless parameter  $\kappa = J/E$  is introduced. This indicates that a massless particle with impact parameter  $b = b_{\pm}(r)$  will have a turning point at the position  $r$ . When the black string is extreme rotating, i.e.  $a = M$ , then  $b_+(r)$  starts from  $2M$  independently of the value of  $\kappa$  and will increase to the infinity with increasing of radial coordinate  $r$ .  $b_-(r)$  starts from  $2M$  which is larger than  $b_+(r)$  and will increase to the infinity with the increase of radial coordinate  $r$ . As radial coordinate increases above  $2M$  to the infinity  $b_-(r)$  starts from the negative infinity and increases to some maximum then monotonically decreases to the negative infinity.

If  $b_{-\max} < b < 2M$  then the particle will escape to infinity if it is moving outward initially. If  $b > 2M$  or  $b < b_{-\max}$  then the particle eventually will escape to infinity independently of the sign of the initial velocity, for the case when it is outside the outer turning point. If  $b = 2M$  or  $b = b_{-\max}$  then the particle will escape to infinity, for the case when it is initially moving outside the turning point.

In the Fig. 19 the radial dependence of the impact parameter  $b_{\pm}$  for the different values of the parameter  $\kappa$  are shown. From the figure one can see that with increasing the value of  $\kappa$  the interval of impact parameter for capturing the massless particles is decreased.

In the Table I the values of local maximum of  $b_-$  are listed. From the results one can see increase of the value

of  $b_{-\max}$  with increase of parameter  $\kappa$  which corresponds to decreasing the interval of impact parameter for capturing massless particles.

Recall for massive particles  $\mathcal{E} = E/m$ ,  $\mathcal{L} = L/(mM)$ , and  $\mathcal{J} = J/m$ . Solving equation  $V(r) = 0$  for massive particle one can obtain

$$\begin{aligned} \mathcal{L} &= \mathcal{L}_{\pm}(r) \\ &= \frac{-2aM\mathcal{E} \pm r\sqrt{\Delta(r)[\mathcal{E}^2 - (1 - 2M/r)(1 + \mathcal{J}^2)]}}{M(r - 2M)}. \end{aligned} \quad (97)$$

Now one may conclude that a massive particle with angular momentum  $\mathcal{L} = \mathcal{L}_{\pm}(r)$  has a turning point at the position  $r$ . For bound orbits, i.e.  $\mathcal{E} < 1 + \mathcal{J}^2$ ,  $V(r)$  is positive as radial coordinate increases to higher values, showing that they are not able to reach infinity but will return back. Thus one may concentrate on soft bound and unbound orbits i.e.  $\mathcal{E} \geq 1 + \mathcal{J}^2$ .

Consider the collision of particles 1 and 2 and creation of particles 3 and 4. The local conservation of four-momentum after the collision is given by

$$p_1^{\alpha} + p_2^{\alpha} = p_3^{\alpha} + p_4^{\alpha}, \quad (98)$$

and if  $\alpha = t$  and  $\alpha = \varphi$  one gets conservation of energy and angular momentum during the reaction.

For the particles 1 and 2 the masses and energies are defined and  $m_3$ ,  $E_3$  and  $L_3$  are specified, then one can determine  $m_4$ ,  $E_4$ , and  $L_4$ . In fact  $m_4$  can be expressed in terms of the quantities of other three particles as follows

$$m_4^2 = -p_{4\alpha}p_4^{\alpha} = -(p_1^{\alpha} + p_2^{\alpha} - p_3^{\alpha})(p_{1\alpha} + p_{2\alpha} - p_{3\alpha}) \quad (99)$$

The CM energy of particles 1 and 2 near the event horizon for a extreme rotating black hole has the following form

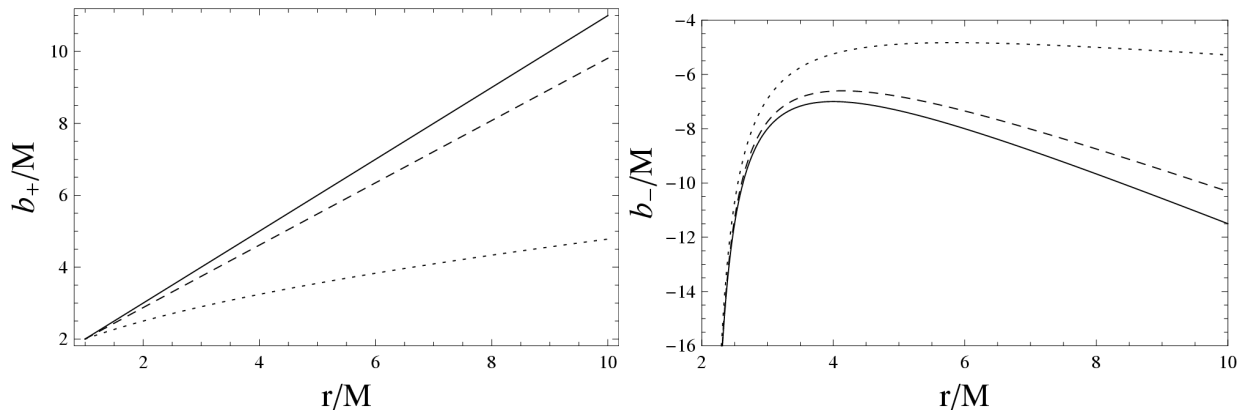
$$\frac{E_{\text{cm}}}{m} \approx \sqrt{\frac{2(2\mathcal{E}_2 - \mathcal{L}_2)(2\mathcal{E}_1 - \sqrt{3\mathcal{E}_1^2 - 1 - \mathcal{J}_1^2})}{\epsilon}}, \quad (100)$$

where we denote the radius of the collision point as  $r_c = M/(1 - \epsilon)$  and  $0 < \epsilon \ll 1$ . For a critical particle, condition



Table I: The values of local maximum of the impact parameter  $b_-$  for the different values of parameter  $\kappa$ .

$\kappa$	0	0.1	0.2	0.3	0.4	0.5	0.6	0.7	0.8	0.9	1.0
$b_{-\max}/M$	-7.0	-6.985	-6.939	-6.862	-6.751	-6.603	-6.412	-6.168	-5.857	-5.444	-4.828
$r/M$	4.0	4.005	4.02	4.048	4.089	4.147	4.231	4.354	4.545	4.887	5.829

Figure 19: The radial dependence of impact parameters for the different values of  $\kappa$ . The solid, dashed, and dotted lines correspond to values of  $j = 0$ ,  $j = 0.5$ , and  $j = 1$ , respectively.

$\mathcal{E}_1 > 1/\sqrt{3}$  must be satisfied. As  $\epsilon \rightarrow 0$ , the CM energy is diverging.

Using the conservation law (98) and considering the particle 3 as escaping, the upper limits of the mass and energy of the emitted particle are given as

$$m_3 \leq (2E_1 - \sqrt{3E_1^2 - m_1^2 - J_1^2})/(2 - \sqrt{2}) = m_B \quad (101)$$

and

$$E_3 \leq (2E_1 - \sqrt{3E_1^2 - m_1^2 - J_1^2})/(2 - \sqrt{3}) = E_B, \quad (102)$$

respectively. Note that  $\lambda_+ = E_B$  can be realised only if particle 3 is massless. Figure 20 shows the upper limits as function of  $E_1/m_1$ . One can easily see that the presence of parameter  $\mathcal{J}$  increases the upper limit of energy of extracted particle.

Using the above result one can easily constrain the efficiency of the energy extraction. The unconditional upper limit is given by

$$\eta_B = \frac{\lambda}{m_1 + m_2} = \frac{(\sqrt{2} + 1)\lambda}{\sqrt{2}m_1 + \lambda},$$

where  $\lambda = (2E_1 - \sqrt{3E_1^2 - m_1^2 - J_1^2})/(2 - \sqrt{3})$ .

Since  $\lambda$  takes the upper limit for  $m_3 = 0$  the unconditional upper limit will depend on the value of  $J_1$ . In the Table II the dependence of energy extraction efficiency for the different values of  $\mathcal{J}$  is shown. One can see that the maximal energy extraction can be increased up to 203.%

## VI. CONCLUSION

In this paper we have studied the effect of the high center-of-mass energy of the collision of two test particles of the same mass in the spacetimes of (i) the static black string, (ii) rotating black string and (iii) the black string immersed in external magnetic field.

The model considered here, the 4D Kerr spacetime with a flat additional dimension, is not an exact solution of the Einstein equations; therefore, a curved spacetime in the additional dimension has to be expected in realistic situations when the spacetime is expected to be an exact solution of the Einstein equations, or their modifications. However, this model can be useful, at least, at the moment of collision of the particles and can represent (locally) the outcome of the collision, since locally the spacetime can be always approximated by the flat geometry. Thus, one can describe the local influence of the additional dimension, e.g., the leaking or appearance of unlimited energy after the collision.

In particular we have shown that the BSW mechanism originally investigated in  $S^2$  topology can be extended to  $S^2 \times \mathbb{R}^1$  topology. We have shown that due to the particular property of the motion in black string spacetime, namely, the appearance of new integral of motion  $J$ , leads to increase of the energy of the particle and as a result increases the maximal center-of-mass energy of the collision of particles. We have demonstrated that there exists a critical angular momentum of a freely falling particle to achieve a horizon of black string and found that when the extra dimension is added, the absolute values of the critical angular momenta increase for any value of the spin parameter  $a$ .

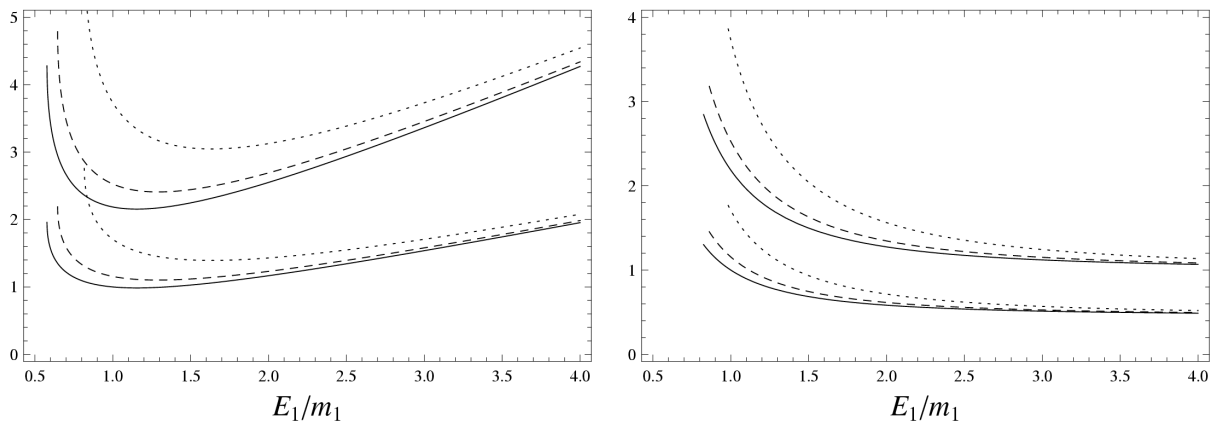


Figure 20: Upper limits of the mass and energy of the emitted particle as functions of the energy of the incident critical particle. The solid, dashed, and dotted lines correspond to the values of  $\mathcal{J} = 0$ ,  $\mathcal{J} = 0.5$ , and  $\mathcal{J} = 1$ , respectively.

Table II: The values of the energy extraction efficiency parameter.

$\mathcal{J}$	0	0.2	0.4	0.6	0.8	0.9	1	1.1	1.2	1.3	1.41
$\eta$	1.46	1.48	1.52	1.58	1.66	1.70	1.75	1.80	1.85	1.91	2.03

We have demonstrated that the center-of-mass energy can be high for a collision of a particle falling from infinity with a charged particle moving at ISCO. In fact, this energy formally infinitely grows when the ISCO shifts arbitrarily close to the horizon which is the result of the influence of the Lorentz force acting on the charged particle. However this energy cannot be unlimited for realistic magnetic fields since the estimated values of the strength of the magnetic fields in relativistic astrophysics are restricted by values  $B \sim 10^8 Gs$  for the stellar mass black holes and  $B \sim 10^4 Gs$  for the supermassive black holes [30].

It has been shown that the collisional energy of particles can be ultrahigh not only for extremely rotating black string, but also when the rotation of the black string is not maximal,  $a < 1$ , if to take into account the probability of the multiple scattering of a freely falling particle with particles from the accretion disc. In the calculation of such a process we used a simplified model where the gravitational field of the accretion disc has been considered infinitely small in comparison with the gravitation of the black string and has not been taken into account.

The frame-dragging effects in a 4D Kerr black hole spacetime can accelerate particles and one needs significant fine-tuning to get sensible cross sections for particles (at least one of particles has to have critical angular momentum). Here we show that in the case of black string we still have fine-tuning but the fine-tuned value of critical angular momentum depends on a new constant of

motion appearing due to the extra dimension. The increase of critical angular momentum in the background 5D black string spacetime is accompanied by a decrease of stability of the particle's trajectories.

We have also analyzed the energy extraction from rotating black string. In the case of an extreme rotating black hole the energy extraction efficiency has the upper limit 146%. We have shown that the presence of the extra dimension can, in principle, increase the upper limit of efficiency of energy extraction up to 203%.

### Acknowledgments

The authors would like to express their acknowledgements for the institutional support of the Faculty of Philosophy and Science of the Silesian University at Opava, the internal student grant of the Silesian University SGS/23/2013 and EU grant Synergy CZ.1.07/2.3.00/20.0071. A. A. and B. A. thank the TIFR, IUCAA (India), and Max Planck Institut für Gravitationsphysik (Albert Einstein Institute, Germany) for warm hospitality. This research is supported in part by the projects F2-FA-F113, FE2-FA-F134, F2-FA-F029 of the UzAS; by the TWAS associateship grants; by the ICTP through the OEA-NET-76, OEA-PRJ-29 projects; and the Volkswagen Stiftung (Grant No. 86 866).

[1] M. Bondarescu “Simple solutions to the Einstein Equations in spaces with unusual topology,” hep-th/0504057

- [2] G. T. Horowitz “Playing with Black Strings,” hep-th/0205069 (2002).
- [3] S. Grunau and B. Khamesra “Geodesic motion in the (rotating) black string spacetime,” arXiv:1303.6863 [gr-qc] (2013).
- [4] A.N. Aliev, A.E. Gumrukcuoglu, “Charged rotating black holes on a 3-brane,” Physical Review D **71**, 104027 (2005).
- [5] J. Schee, Z. Stuchlik, “Optical phenomena in the field of braneworld Kerr black holes,” Int. Journal of Modern Physics D **18** 983- (2009)
- [6] Z. Stuchlik, “Equatorial circular orbits and the motion of the shell of dust in the field of a rotating naked singularity,” Bulletin of the Astronomical Institutes of Czechoslovakia, **31**, 129 (1980).
- [7] S. Pal and S. Kar, “Gravitational lensing in braneworld gravity: formalism and applications,” Class. Quantum Grav., **25**, 045003 (2008)
- [8] A. A. Abdujabbarov and B. J. Ahmedov, “Test particle motion around a black hole in a braneworld,” Phys. Rev. D **81**, 044022 (2010)
- [9] J. Schee and Z. Stuchlik, “Profiles of emission lines generated by rings orbiting braneworld Kerr black holes,” Gen. Rel. Gravit., **41**, 1795 (2009)
- [10] Z. Stuchlik and A. Kotrlova, “Orbital resonances in discs around braneworld Kerr black holes,” Gen. Rel. Gravit., **41**, 1305 (2009)
- [11] C.G. Böhrmer, T. Harko, F.S.N. Lobo, “Solar system tests of brane world models,” Class. Quantum Grav. **25**, 045015 (2008)
- [12] C.S.J. Pun, Z. Kovács, T. Harko, “Thin accretion disks onto brane world black holes,” Phys. Rev. D **78**, 084015 (2008)
- [13] E. Hackman, V. Kagramanova, J. Kunz, C. Lämmerzahl, “Analytic solutions of the geodesic equation in higher dimensional static spherically symmetric spacetimes,” Phys. Rev. D **78**, 124018 (2008)
- [14] A. N. Aliev and D. V. Galtsov, “Gravitational Effects in the Field of a Central Body Threaded by a Cosmic String,” Sov. Astron. Lett. **14**, 48 (1988).
- [15] D. V. Galtsov and E. Masar, “Geodesics In Space-times Containing Cosmic Strings,” Class. Quant. Grav. **6**, 1313 (1989).
- [16] S. Chakraborty and L. Biswas, “Motion of test particles in the gravitational field of cosmic strings in different situations,” Class. Quant. Grav. **13**, 2153 (1996).
- [17] N. Ozdemir, “Gravitomagnetic effects and cosmic strings,” Class. Quant. Grav. **20**, 4409 (2003).
- [18] F. Ozdemir, N. Ozdemir and B. T. Kaynak, “Multi-black holes solution with cosmic strings,” Int. J. Mod. Phys. A **19**, 1549 (2004).
- [19] E. Hackmann, B. Hartmann, C. Lämmerzahl and P. Sirimachan, “The Complete set of solutions of the geodesic equations in the space-time of a Schwarzschild black hole pierced by a cosmic string,” Phys. Rev. D **81**, 064016 (2010) [arXiv:0912.2327 [gr-qc]].
- [20] E. Hackmann, B. Hartmann, C. Lämmerzahl and P. Sirimachan, “Test particle motion in the space-time of a Kerr black hole pierced by a cosmic string,” Phys. Rev. D **82**, 044024 (2010) [arXiv:1006.1761 [gr-qc]].
- [21] B. Hartmann and P. Sirimachan, “Geodesic motion in the space-time of a cosmic string,” JHEP **1008**, 110 (2010) [arXiv:1007.0863 [gr-qc]].
- [22] B. Hartmann and V. Kagramanova, “Geodesic motion in the space-time of cosmic strings interacting via magnetic fields,” Phys. Rev. D **86**, 045028 (2012) [arXiv:1204.0396 [hep-th]].
- [23] B. Hartmann, C. Lämmerzahl and P. Sirimachan, “Detection of cosmic superstrings by geodesic test particle motion,” Phys. Rev. D **83**, 045027 (2011) [arXiv:1012.3285 [hep-th]].
- [24] M. Bañados, J. Silk and S. M. West, “Kerr Black Holes as Particle Accelerators to Arbitrarily High Energy,” Phys. Rev. Lett. **103**, 111102 (2009)
- [25] J. L. Said and K. Z. Adami, “Rotating charged cylindrical black holes as particle accelerators,” Phys. Rev. D **83**, 104047 (2011)
- [26] T. Jacobson and T. P. Sotiriou, “Spinning Black Holes as Particle Accelerators,” Phys. Rev. Lett. **104**, 021101 (2010)
- [27] O. B. Zaslavsky, “Acceleration of particles by rotating black holes: near-horizon geometry and kinematics,” Grav. Cosmol. **18**, 139 (2012)
- [28] V. P. Frolov and A. A. Shoom, “Motion of charged particles near weakly magnetized Schwarzschild black hole,” Phys. Rev. D **82**, 084034 (2010)
- [29] R.M. Wald, “Black hole in a uniform magnetic field,” Phys. Rev. D **10**, 1680 (1974).
- [30] V. P. Frolov, “Weakly magnetized black holes as particle accelerators,” Phys. Rev. D **85**, 024020 (2012)
- [31] A. A. Abdujabbarov, A. A. Tursunov, B. J. Ahmedov and A. Kuvatov, “Acceleration of particles by black hole with gravitomagnetic charge immersed in magnetic field,” Astrophys. Space. Sci. **343**, 173 (2013)
- [32] A. A. Abdujabbarov, B. J. Ahmedov and N. B. Jurayeva, “Charged-particle motion around a rotating non-Kerr black hole immersed in a uniform magnetic field,” Phys. Rev. D **87**, 064042 (2013)
- [33] M. Patil and P. Joshi, “Kerr naked singularities as particle accelerators,” Class. Quantum Grav. **28** 235012 (2011)
- [34] Z. Stuchlík, S. Hledík and K. Truparová, “Evolution of Kerr superspinars due to accretion counterrotating Keplerian discs,” Class. Quantum Grav. **28** 155017 (2011)
- [35] Z. Stuchlík and J. Schee, “Observational phenomena related to primordial Kerr superspinars,” Class. Quantum Grav. **29** 065002 (2012)
- [36] Z. Stuchlík and J. Schee, “Counter-rotating Keplerian discs around Kerr superspinars,” Class. Quantum Grav. **29** 025008 (2012)
- [37] Z. Stuchlík and J. Schee, “Ultra-high-energy collisions in the superspinning Kerr geometry,” Class. Quantum Grav. **30** 075012 (2013)
- [38] Z. Stuchlík and J. Schee, “Appearance of Keplerian discs orbiting Kerr superspinars,” Class. Quantum Grav. **27**, 215017 (2010).
- [39] F. Atamurotov, B. Ahmedov and S. Shaymatov, “Formation of black holes through BSW effect and black hole-black hole collisions,” Astrophys. Space. Sci. **347**, 277 (2013)
- [40] L. Rezzolla, K. Takami, “Black-hole production from ultrarelativistic collisions,” Class. Quantum Grav., **30**, 012001 (2013).
- [41] T. Harada, M. Kimura, “Collision of an innermost stable circular orbit particle around a Kerr black hole,” Physical Review D, **83**, 024002 (2011).
- [42] T. Harada, M. Kimura, “Collision of two general geodesic particles around a Kerr black hole” Physical Review D,

- 83**, 084041 (2011).
- [43] N. Tsukamoto, M. Kimura, T. Harada, “High Energy Collision of Particles in the Vicinity of Extremal Black Holes in Higher Dimensions: Banados-Silk-West Process as Linear Instability of Extremal Black Holes,” arXiv:1310.5716 (2013).
- [44] H. Nemoto, U. Miyamoto, T. Harada, T. Kokubu, “Escape of superheavy and highly energetic particles produced by particle collisions near maximally charged black holes,” *Physical Review D*, **87**, 127502 (2013).
- [45] T. Harada, H. Nemoto, U. Miyamoto, “Upper limits of particle emission from high-energy collision and reaction near a maximally rotating Kerr black hole,” *Physical Review D*, **86**, 024027 (2012).
- [46] A. Abdujabbarov, N. Dadhich, B. Ahmedov, H. Eshkuvatov, “Particle acceleration around a five-dimensional Kerr black hole,” *Physical Review D* **88**, 084036 (2013).
- [47] B. O’Neill, “The Geometry of Kerr Black Holes”, AK Peters, Wellesley, Massachusetts, (1995).
- [48] S. Gao and C. Zhong, “Non-extremal Kerr black holes as particle accelerators,” *Phys. Rev. D* **84**, 044006 (2011) [arXiv:1106.2852 [gr-qc]].
- [49] A. A. Grib and Yu. V. Pavlov, “On particle collisions near rotating black holes,” *Grav. and Cosmol.* **17**, 42 (2011)
- [50] K. S. Thorne, “Disk Accretion onto a Black Hole. II. Evolution of the Hole,” *Astrophys. J.* **191**, 507 (1974).